Published September 16, 2013

extracted in lysis buffer (50 mM Hepes-NaOH, pH 7.5, containing 150 mM NaCl, 1% Nonidet P-40, 20 mM NEM, and protease inhibitors) and centrifuged at 15,000 *g* for 20 min at 4°C. The supernatants were used for immunoblotting, for immunoprecipitation of FLAG-tagged oxidoreductases with anti-FLAG M2-agarose beads (Sigma-Aldrich; 1), or for immunoprecipitation of endogenous Ero1-α with Con A–Sepharose 4B (GE Healthcare; 2). Bead suspensions were rotated for 3 h at 4°C. After precipitation, the beads were washed three times with lysis buffer and eluted by adding lysis buffer containing 0.2 mg/ml FLAG peptide for 1 or by denaturing with SDS-PAGE sample buffer containing 5 mM EDTA for 2. Immunoblotting was conducted under reducing or nonreducing conditions with specific antibodies as indicated in the text (Results section Ero1-α is dominantly regulated by PDI).

SPR measurements

The SPR analysis was performed essentially as described previously (Araki and Nagata, 2011a). In brief, association or dissociation rate constants (k_{on} or k_{off}) for the direct binding of oxidoreductases to immobilized Ero1-α(WT) were determined by SPR measurements on a protein interaction array system (ProteOn XPR36; Bio-Rad Laboratories). Ero1-α(WT) was coupled to the GLC (general amine coupling, compact polymer layer) sensor chip (Bio-Rad Laboratories) through amine-coupling chemistry. As a control, one channel was coupled with BSA to exclude background binding. Sensorgrams were recorded simultaneously for five concentrations of purified oxidoreductases (0.133–36 µM) in threefold increments at 25°C for a 2-min association phase followed by a 10-min dissociation phase with 20 mM Hepes-NaOH, pH 7.4, 150 mM NaCl, 0.001% Tween, and 2 mM EDTA as running and sample buffers. GSH or GSSG (final 2 mM GSH and 0.5 mM GSSG) were added to the running buffer just before use, and all samples were exchanged and diluted in this buffer. Sensorgrams were analyzed by nonlinear regression analysis according to a two-state model using ProteOn Manager Version 3.0 software (Bio-Rad Laboratories). Experiments were replicated at least three times.

Oxygen consumption assays

Oxygen consumption was measured using a Clark-type oxygen electrode (YSI 5331) as previously described (Araki and Nagata, 2011a). In brief, all experiments were performed at 25°C using a constant temperature incubator in air-saturated buffer (~250 µM O_2) in 50 mM Hepes-NaOH, pH 7.5, 150 mM NaCl, and 2 mM EDTA. Catalytic oxygen consumption was initiated by the addition of Ero1-α(WT) or Ero1-α(C104A/C131A) at a final concentration of 2 µM in a reaction mixture containing 10 mM GSH and various concentrations of oxidoreductases as depicted in each figure.

NMR measurements

E. coli cells were grown in M9 minimal media containing 25 mg/liter L-[1-^{13}C]cysteine, either with or without 100 mg/liter L-[^{15}N]alanine or 200 mg/liter L-[^{15}N]glycine, to produce isotopically labeled constitutively active Ero1-α(C104A/C131A). NMR measurements were made on a research spectrometer (AVANCE III-400; Bruker) at 303 K with a 5-mm NMR sample tube, which contained 0.85 mM Ero1-α(C104A/C131A) dissolved in 10 mM sodium phosphate buffer containing 100 mM NaCl, pH 7.0. ^{13}C NMR spectra were recorded at 100 MHz with a WALTZ-16 composite pulse decoupling sequence. The free induction decay was recorded with 32 K data points and a spectral width of 3,500 Hz. Carbonyl ^{13}C signals were assigned by the selective ^{13}C carbonyl-^{15}N double-labeling method (Serve et al., 2010). The ^{13}CO-^{15}N linkages in the polypeptide chains of the doubly labeled proteins are used to give the carbonyl ^{13}C resonances that split into doublets as a result of the ^{13}C-^{15}N spin coupling (Kainosho and Tsuji, 1982). Thus, one can sort out the carbonyl ^{13}C resonances caused by the amino acid residues that possess a ^{13}CO-^{15}N linkage. If there is only one ^{13}CO-^{15}N linkage in a protein molecule, it is possible to unambiguously assign the carbonyl ^{13}C resonance to the specific amino acid residue on the basis of knowledge of the amino acid sequence of the protein. For example, Cys94 of Ero1-α was assigned by the double-labeled Ero1-α in which the carbonyl carbon of cysteine (Cys94) and the nitrogen of glycine (Gly95) because the Cys-Gly linkage exists only here in the Ero1-α protein sequence. To subtract the signal of the natural isotope abundance, the spectrum of the unlabeled protein was subtracted from that of the labeled one. All data were collected and processed under the same experimental condition, and the y axis indicates relative intensity (arbitrary unit).

Measurement of redox equilibrium using glutathione

The redox equilibrium between recombinant oxidoreductases and glutathione was measured essentially as described previously (Sugiura et al., 2010). In brief, oxidoreductases (1 µM) were incubated with 0.1 mM GSSG and various concentrations of GSH at 25°C for 1 h in 0.1 M sodium phosphate buffer, pH 7.0, containing 1 mM EDTA and 150 mM NaCl. After incubation, 10% TCA was added to prevent further thiol–disulfide exchange. The precipitated pellet was washed with 100% acetone and solubilized in 0.1 M sodium phosphate buffer, pH 7.0, containing 2% SDS and 3 mM methoxypolyethylene glycol (mean molecular weight of 2,000)-maleimide (mPEG2000-mal; Sunbright ME-020MA, NOF Corporation). The mixture was incubated at 25°C for 30 min to alkylate the free sulfhydryl groups of cysteines. Samples were separated by SDS-PAGE and stained with Coomassie brilliant blue (CBB). Values for the reduced form fraction were quantified by measuring the PEG2000-induced mobility from the complete oxidized state as shown in Fig. S4. After quantification, the values for the completely oxidized or reduced states were regarded as 0 or 1, respectively, and all intermediate states were recalibrated. The redox equilibrium constant (K_{eq}) was calculated by fitting the recalibrated fraction of the apparent reduced form to the following equation: $R = \{[GSH]^2/[GSSG]\}/\{K_{eq} + ([GSH]^2/[GSSG])\}$, in which R is the relative ratio of reduced oxidoreductases.

Online supplemental material

Fig. S1 shows that Ero1-α binds to ER-resident oxidoreductases. Fig. S2 shows validation of siRNA silencing and annotation of Cys94 with a double-labeling method. Fig. S3 shows PDI(AA) does not accelerate the Ero1-α oxidation system. Fig. S4 shows the method used to calculate the K_{eq} values. Table S1 shows a list of publications reporting Ero1-α–related assays and having a bearing on this study. Online supplemental material is available at http://www.jcb.org/cgi/content/full/jcb.201303027/DC1.

We thank Ryota Maeda and Yo-ichi Nabeshima for allowing us to use their SPR system. We thank Koreaki Ito for his critical reading of the manuscript and valuable suggestions. We thank Lars Ellgaard for sharing his work before publication and for providing informative suggestions.

This work was supported by a Grant-in-Aid for Creative Scientific Research (19G0314) and for Scientific Research on Priority Area (19058008) from the Ministry of Education, Culture, Sports, Science and Technology (to K. Nagata), Grants-in-Aid for Scientific Research on Innovative Areas (25102008), for Scientific Research (24249002), and partly, Nanotechnology Platform Program from the Ministry of Education, Culture, Sports, Science and Technology (to K. Kato), a Grant-in-Aid for Scientific Research on Priority Areas (22020039; to Y. Kamiya), the New Energy and Industrial Technology Development Organization (to T. Natsume), and a fellowship from the Japan Society for the Promotion of Science (to K. Araki). D. Ron is a Wellcome Trust Principal Research Fellow.

Submitted: 6 March 2013
Accepted: 8 August 2013

References

Anelli, T., M. Alessio, A. Bachi, L. Bergamelli, G. Bertoli, S. Camerini, A. Mezghrani, E. Ruffato, T. Simmen, and R. Sitia. 2003. Thiol-mediated protein retention in the endoplasmic reticulum: the role of ERp44. *EMBO J.* 22:5015–5022. http://dx.doi.org/10.1093/emboj/cdg491

Appenzeller-Herzog, C., and L. Ellgaard. 2008. The human PDI family: versatility packed into a single fold. *Biochim. Biophys. Acta.* 1783:535–548. http://dx.doi.org/10.1016/j.bbamcr.2007.11.010

Appenzeller-Herzog, C., J. Riemer, B. Christensen, E.S. Sørensen, and L. Ellgaard. 2008. A novel disulphide switch mechanism in Ero1alpha balances ER oxidation in human cells. *EMBO J.* 27:2977–2987. http://dx.doi.org/10.1038/emboj.2008.202

Appenzeller-Herzog, C., J. Riemer, E. Zito, K.T. Chin, D. Ron, M. Spiess, and L. Ellgaard. 2010. Disulphide production by Ero1α-PDI relay is rapid and effectively regulated. *EMBO J.* 29:3318–3329. http://dx.doi.org/10.1038/emboj.2010.203

Araki, K., and K. Inaba. 2012. Structure, mechanism, and evolution of Ero1 family enzymes. *Antioxid. Redox Signal.* 16:790–799. http://dx.doi.org/10.1089/ars.2011.4418

Araki, K., and K. Nagata. 2011a. Functional in vitro analysis of the ERO1 protein and protein-disulfide isomerase pathway. *J. Biol. Chem.* 286:32705–32712. http://dx.doi.org/10.1074/jbc.M111.227181

Araki, K., and K. Nagata. 2011b. Protein folding and quality control in the ER. *Cold Spring Harb. Perspect. Biol.* 3:a007526. http://dx.doi.org/10.1101/cshperspect.a007526

Baker, K.M., S. Chakravarthi, K.P. Langton, A.M. Sheppard, H. Lu, and N.J. Bulleid. 2008. Low reduction potential of Ero1alpha regulatory disulphides

ensures tight control of substrate oxidation. *EMBO J.* 27:2988–2997. http://dx.doi.org/10.1038/emboj.2008.230

Bánhegyi, G., J. Mandl, and M. Csala. 2008. Redox-based endoplasmic reticulum dysfunction in neurological diseases. *J. Neurochem.* 107:20–34. http://dx.doi.org/10.1111/j.1471-4159.2008.05571.x

Benham, A.M. 2012. The protein disulfide isomerase family: key players in health and disease. *Antioxid. Redox Signal.* 16:781–789. http://dx.doi.org/10.1089/ars.2011.4439

Benham, A.M., A. Cabibbo, A. Fassio, N. Bulleid, R. Sitia, and I. Braakman. 2000. The CXXCXXC motif determines the folding, structure and stability of human Ero1-Lalpha. *EMBO J.* 19:4493–4502. http://dx.doi.org/10.1093/emboj/19.17.4493

Chambers, J.E., T.J. Tavender, O.B. Oka, S. Warwood, D. Knight, and N.J. Bulleid. 2010. The reduction potential of the active site disulfides of human protein disulfide isomerase limits oxidation of the enzyme by Ero1α. *J. Biol. Chem.* 285:29200–29207. http://dx.doi.org/10.1074/jbc.M110.156596

Dixon, B.M., S.H. Heath, R. Kim, J.H. Suh, and T.M. Hagen. 2008. Assessment of endoplasmic reticulum glutathione redox status is confounded by extensive ex vivo oxidation. *Antioxid. Redox Signal.* 10:963–972. http://dx.doi.org/10.1089/ars.2007.1869

Ellgaard, L., and L.W. Ruddock. 2005. The human protein disulphide isomerase family: substrate interactions and functional properties. *EMBO Rep.* 6:28–32. http://dx.doi.org/10.1038/sj.embor.7400311

Freedman, R.B., T.R. Hirst, and M.F. Tuite. 1994. Protein disulphide isomerase: building bridges in protein folding. *Trends Biochem. Sci.* 19:331–336. http://dx.doi.org/10.1016/0968-0004(94)90072-8

Frickel, E.M., P. Frei, M. Bouvier, W.F. Stafford, A. Helenius, R. Glockshuber, and L. Ellgaard. 2004. ERp57 is a multifunctional thiol-disulfide oxidoreductase. *J. Biol. Chem.* 279:18277–18287. http://dx.doi.org/10.1074/jbc.M314089200

Gross, E., C.S. Sevier, N. Heldman, E. Vitu, M. Bentzur, C.A. Kaiser, C. Thorpe, and D. Fass. 2006. Generating disulfides enzymatically: reaction products and electron acceptors of the endoplasmic reticulum thiol oxidase Ero1p. *Proc. Natl. Acad. Sci. USA.* 103:299–304. http://dx.doi.org/10.1073/pnas.0506448103

Hatahet, F., and L.W. Ruddock. 2007. Substrate recognition by the protein disulfide isomerases. *FEBS J.* 274:5223–5234. http://dx.doi.org/10.1111/j.1742-4658.2007.06058.x

Hatahet, F., and L.W. Ruddock. 2009. Protein disulfide isomerase: a critical evaluation of its function in disulfide bond formation. *Antioxid. Redox Signal.* 11:2807–2850. http://dx.doi.org/10.1089/ars.2009.2466

Hebert, D.N., and M. Molinari. 2007. In and out of the ER: protein folding, quality control, degradation, and related human diseases. *Physiol. Rev.* 87:1377–1408. http://dx.doi.org/10.1152/physrev.00050.2006

Inaba, K., S. Murakami, M. Suzuki, A. Nakagawa, E. Yamashita, K. Okada, and K. Ito. 2006. Crystal structure of the DsbB-DsbA complex reveals a mechanism of disulfide bond generation. *Cell.* 127:789–801. http://dx.doi.org/10.1016/j.cell.2006.10.034

Inaba, K., S. Murakami, A. Nakagawa, H. Iida, M. Kinjo, K. Ito, and M. Suzuki. 2009. Dynamic nature of disulphide bond formation catalysts revealed by crystal structures of DsbB. *EMBO J.* 28:779–791. http://dx.doi.org/10.1038/emboj.2009.21

Inaba, K., S. Masui, H. Iida, S. Vavassori, R. Sitia, and M. Suzuki. 2010. Crystal structures of human Ero1α reveal the mechanisms of regulated and targeted oxidation of PDI. *EMBO J.* 29:3330–3343. http://dx.doi.org/10.1038/emboj.2010.222

Jessop, C.E., S. Chakravarthi, N. Garbi, G.J. Hämmerling, S. Lovell, and N.J. Bulleid. 2007. ERp57 is essential for efficient folding of glycoproteins sharing common structural domains. *EMBO J.* 26:28–40. http://dx.doi.org/10.1038/sj.emboj.7601505

Jessop, C.E., T.J. Tavender, R.H. Watkins, J.E. Chambers, and N.J. Bulleid. 2009a. Substrate specificity of the oxidoreductase ERp57 is determined primarily by its interaction with calnexin and calreticulin. *J. Biol. Chem.* 284:2194–2202. http://dx.doi.org/10.1074/jbc.M808054200

Jessop, C.E., R.H. Watkins, J.J. Simmons, M. Tasab, and N.J. Bulleid. 2009b. Protein disulphide isomerase family members show distinct substrate specificity: P5 is targeted to BiP client proteins. *J. Cell Sci.* 122:4287–4295. http://dx.doi.org/10.1242/jcs.059154

Kainosho, M., and T. Tsuji. 1982. Assignment of the three methionyl carbonyl carbon resonances in *Streptomyces* subtilisin inhibitor by a carbon-13 and nitrogen-15 double-labeling technique. A new strategy for structural studies of proteins in solution. *Biochemistry.* 21:6273–6279. http://dx.doi.org/10.1021/bi00267a036

Kim, H., C. Matsunaga, A. Yoshino, K. Kato, and Y. Arata. 1994. Dynamical structure of the hinge region of immunoglobulin G as studied by 13C nuclear magnetic resonance spectroscopy. *J. Mol. Biol.* 236:300–309. http://dx.doi.org/10.1006/jmbi.1994.1136

Lundström, J., and A. Holmgren. 1993. Determination of the reduction-oxidation potential of the thioredoxin-like domains of protein disulfide-isomerase from the equilibrium with glutathione and thioredoxin. *Biochemistry.* 32:6649–6655. http://dx.doi.org/10.1021/bi00077a018

Masui, S., S. Vavassori, C. Fagioli, R. Sitia, and K. Inaba. 2011. Molecular bases of cyclic and specific disulfide interchange between human ERO1alpha protein and protein-disulfide isomerase (PDI). *J. Biol. Chem.* 286:16261–16271. http://dx.doi.org/10.1074/jbc.M111.231357

Matsunaga, C., K. Kato, and Y. Arata. 1991. A 13C NMR study of the hinge region of a mouse monoclonal antibody. *J. Biomol. NMR.* 1:379–390. http://dx.doi.org/10.1007/BF02192861

Morjana, N.A., and H.F. Gilbert. 1991. Effect of protein and peptide inhibitors on the activity of protein disulfide isomerase. *Biochemistry.* 30:4985–4990. http://dx.doi.org/10.1021/bi00234a021

Nakasako, M., A. Maeno, E. Kurimoto, T. Harada, Y. Yamaguchi, T. Oka, Y. Takayama, A. Iwata, and K. Kato. 2010. Redox-dependent domain rearrangement of protein disulfide isomerase from a thermophilic fungus. *Biochemistry.* 49:6953–6962. http://dx.doi.org/10.1021/bi1006089

Natsume, T., Y. Yamauchi, H. Nakayama, T. Shinkawa, M. Yanagida, N. Takahashi, and T. Isobe. 2002. A direct nanoflow liquid chromatography-tandem mass spectrometry system for interaction proteomics. *Anal. Chem.* 74:4725–4733. http://dx.doi.org/10.1021/ac020018n

Riemer, J., N. Bulleid, and J.M. Herrmann. 2009. Disulfide formation in the ER and mitochondria: two solutions to a common process. *Science.* 324:1284–1287. http://dx.doi.org/10.1126/science.1170653

Rutkevich, L.A., and D.B. Williams. 2012. Vitamin K epoxide reductase contributes to protein disulfide formation and redox homeostasis within the endoplasmic reticulum. *Mol. Biol. Cell.* 23:2017–2027. http://dx.doi.org/10.1091/mbc.E12-02-0102

Rutkevich, L.A., M.F. Cohen-Doyle, U. Brockmeier, and D.B. Williams. 2010. Functional relationship between protein disulfide isomerase family members during the oxidative folding of human secretory proteins. *Mol. Biol. Cell.* 21:3093–3105. http://dx.doi.org/10.1091/mbc.E10-04-0356

Serve, O., Y. Kamiya, A. Maeno, M. Nakano, C. Murakami, H. Sasakawa, Y. Yamaguchi, T. Harada, E. Kurimoto, M. Yagi-Utsumi, et al. 2010. Redox-dependent domain rearrangement of protein disulfide isomerase coupled with exposure of its substrate-binding hydrophobic surface. *J. Mol. Biol.* 396:361–374. http://dx.doi.org/10.1016/j.jmb.2009.11.049

Sevier, C.S., and C.A. Kaiser. 2008. Ero1 and redox homeostasis in the endoplasmic reticulum. *Biochim. Biophys. Acta.* 1783:549–556. http://dx.doi.org/10.1016/j.bbamcr.2007.12.011

Sevier, C.S., H. Qu, N. Heldman, E. Gross, D. Fass, and C.A. Kaiser. 2007. Modulation of cellular disulfide-bond formation and the ER redox environment by feedback regulation of Ero1. *Cell.* 129:333–344. http://dx.doi.org/10.1016/j.cell.2007.02.039

Sugiura, Y., K. Araki, S. Iemura, T. Natsume, J. Hoseki, and K. Nagata. 2010. Novel thioredoxin-related transmembrane protein TMX4 has reductase activity. *J. Biol. Chem.* 285:7135–7142. http://dx.doi.org/10.1074/jbc.M109.082545

Tabas, I., and D. Ron. 2011. Integrating the mechanisms of apoptosis induced by endoplasmic reticulum stress. *Nat. Cell Biol.* 13:184–190. http://dx.doi.org/10.1038/ncb0311-184

Tavender, T.J., and N.J. Bulleid. 2010. Molecular mechanisms regulating oxidative activity of the Ero1 family in the endoplasmic reticulum. *Antioxid. Redox Signal.* 13:1177–1187. http://dx.doi.org/10.1089/ars.2010.3230

Tavender, T.J., J.J. Springate, and N.J. Bulleid. 2010. Recycling of peroxiredoxin IV provides a novel pathway for disulphide formation in the endoplasmic reticulum. *EMBO J.* 29:4185–4197. http://dx.doi.org/10.1038/emboj.2010.273

Ushioda, R., J. Hoseki, K. Araki, G. Jansen, D.Y. Thomas, and K. Nagata. 2008. ERdj5 is required as a disulfide reductase for degradation of misfolded proteins in the ER. *Science.* 321:569–572. http://dx.doi.org/10.1126/science.1159293

van Anken, E., F. Pena, N. Hafkemeijer, C. Christis, E.P. Romijn, U. Grauschopf, V.M. Oorschot, T. Pertel, S. Engels, A. Ora, et al. 2009. Efficient IgM assembly and secretion require the plasma cell induced endoplasmic reticulum protein pERp1. *Proc. Natl. Acad. Sci. USA.* 106:17019–17024. http://dx.doi.org/10.1073/pnas.0903036106

van Lith, M., S. Tiwari, J. Pediani, G. Milligan, and N.J. Bulleid. 2011. Real-time monitoring of redox changes in the mammalian endoplasmic reticulum. *J. Cell Sci.* 124:2349–2356. http://dx.doi.org/10.1242/jcs.085530

Wang, C., J. Yu, L. Huo, L. Wang, W. Feng, and C.C. Wang. 2012. Human protein-disulfide isomerase is a redox-regulated chaperone activated by oxidation of domain a'. *J. Biol. Chem.* 287:1139–1149. http://dx.doi.org/10.1074/jbc.M111.303149

Wang, C., W. Li, J. Ren, J. Fang, H. Ke, W. Gong, W. Feng, and C.C. Wang. 2013. Structural insights into the redox-regulated dynamic conformations of human protein disulfide isomerase. *Antioxid. Redox Signal.* 19:36–45. http://dx.doi.org/10.1089/ars.2012.4630

Published September 16, 2013

Wang, L., S.J. Li, A. Sidhu, L. Zhu, Y. Liang, R.B. Freedman, and C.C. Wang. 2009. Reconstitution of human Ero1-Lalpha/protein-disulfide isomerase oxidative folding pathway in vitro. Position-dependent differences in role between the a and a' domains of protein-disulfide isomerase. *J. Biol. Chem.* 284:199–206. http://dx.doi.org/10.1074/jbc.M806645200

Zhang, K., and R.J. Kaufman. 2008. From endoplasmic-reticulum stress to the inflammatory response. *Nature*. 454:455–462. http://dx.doi.org/10.1038/nature07203

Zhou, Y., T. Cierpicki, R.H. Jimenez, S.M. Lukasik, J.F. Ellena, D.S. Cafiso, H. Kadokura, J. Beckwith, and J.H. Bushweller. 2008. NMR solution structure of the integral membrane enzyme DsbB: functional insights into DsbB-catalyzed disulfide bond formation. *Mol. Cell*. 31:896–908. http://dx.doi.org/10.1016/j.molcel.2008.08.028

Zito, E., E.P. Melo, Y. Yang, A. Wahlander, T.A. Neubert, and D. Ron. 2010. Oxidative protein folding by an endoplasmic reticulum-localized peroxiredoxin. *Mol. Cell*. 40:787–797. http://dx.doi.org/10.1016/j.molcel.2010.11.010

Araki et al., http://www.jcb.org/cgi/content/full/jcb.201303027/DC1

A

Gene_Symbol	Identified Number	Protein Name	1	2	3	4	5	6	7	8
Bait protein	Total 8 trials									
Ero1α	8	ERO1-like	9	10	10	10	10	9	9	5
Ero1α or Ero1β	8	ERO1-like or ERO1-like β	2	2	2	2	2	2	2	2
HIT Preys										
PDI (P4HB)	8	prolyl 4-hydroxylase, β subunit	19	19	19	21	19	20	22	15
ERp57 (PDIA3)	8	protein disulfide-isomerase A3	7	7	7	5	7	7	6	4
ERp72 (PDIA4)	8	protein disulfide isomerase A4	2	3	4	2	1	1	3	3
P5 (PDIA6)	8	protein disulfide isomerase A6	7	6	6	7	7	7	7	5
ERp46 (TXNDC5)	8	thioredoxin domain containing 5	2	2	3	2	2	2	2	2
CANX	8	calnexin	4	4	5	4	1	1	2	2
ERp44 (TXNDC4)	7	thioredoxin domain containing 4 (endoplasmic reticulum)	6	5	6	6	5	5	5	0
EVI5L	6	ecotropic viral integration site 5-like- isoform 2	0	1	0	1	1	1	1	1
SCYL2	6	SCY1-like 2 protein	21	20	19	18	0	0	2	3
CALR	4	calreticulin	4	3	3	2	0	0	0	6
ERdj5 (DNAJC10)	4	Dnad (Hsp40) homologue, subfamily C, member 10	4	5	3	2	0	0	0	0
PRDX4	4	peroxiredoxin 4	0	0	0	0	1	1	1	1
UGCGL1	4	UDP-glucose ceramide glucosyltransferase-like 1; isoform 2	7	5	6	3	0	0	0	0
Total Hit preys	13		16	13	15	14	8	8	12	14

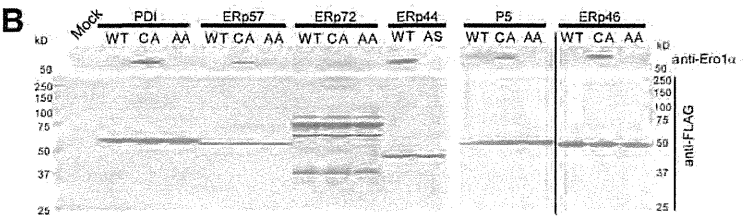

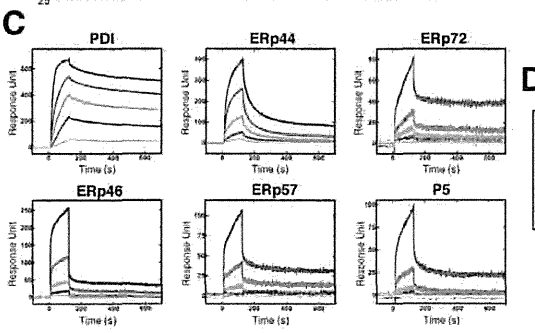

D

	k_{on} ($M^{-1}s^{-1}$)	k_{off} (s^{-1})	K_d (M)
PDI	$2.2\pm0.1\times10^{3}$	$3.9\pm0.1\times10^{-3}$	$1.7\pm0.3\times10^{-6}$
ERp44	$9.8\pm0.4\times10^{2}$	$2.0\pm0.8\times10^{-2}$	$2.1\pm0.6\times10^{-5}$
ERp46	$1.6\pm0.2\times10^{3}$	$4.5\pm0.3\times10^{-1}$	$2.8\pm0.1\times10^{-4}$
ERp72	$1.4\pm1.4\times10^{3}$	$2.2\pm2.4\times10^{-1}$	$1.6\pm9.0\times10^{-4}$
ERp57	$1.7\pm1.1\times10^{3}$	$3.0\pm2.5\times10^{-1}$	$1.8\pm0.6\times10^{-4}$
P5	$3.1\pm1.7\times10^{2}$	$2.2\pm0.4\times10^{-2}$	$7.0\pm0.7\times10^{-5}$

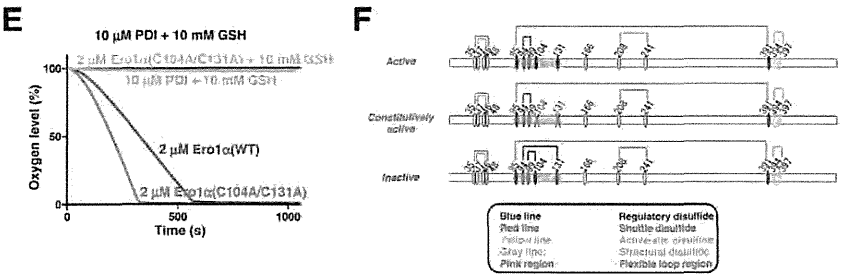

Figure S1. **Ero1-α binds to ER-resident oxidoreductases.** (A) Ero1-α(WT)–FLAG was expressed in HEK293T cells, and anti-FLAG immunoprecipitates were analyzed by direct nanoflow liquid chromatography/tandem mass spectrometry. Preys identified during eight independent trials are listed. Each number indicates the identified peptide number of each protein in individual experiments. Gray bars show the poor reproducible preys or nonoxidoreductases. (B) HEK293T cells were transfected with a series of oxidoreductases, including the wild type (WT) and their mutants (CA and AA), as indicated. Cell lysates were immunoprecipitated by anti-FLAG antibody, subjected to SDS-PAGE on two separate membranes, and analyzed by immunoblotting with anti–Ero1-α (top) and anti-FLAG (bottom) antibodies. A black line on the right indicates the removal of intervening lanes from one of the membranes for presentation purposes. Note that ERp44 contains a CRFS motif in its active site, and its mutant is ARFS (AS). (C) Recombinant Ero1-α(WT) proteins were immobilized on the surface of a sensor chip. Binding responses were collected at five different concentrations (0.444–36 μM, in a threefold dilution series) of oxidoreductases under redox conditions equivalent to those in the ER (GSH/GSSG ratio = 4:1). Association or dissociation rate constants (k_{on} or k_{off}) were determined using a two-state reaction model. (D) SPR-quantified result. Data represent means ± SE from at least three individual experiments. (E) Assays were conducted in a sealed chamber starting with air-saturated buffer containing 10 mM GSH, which was regarded as the 100% oxygen level (~250 μM oxygen). Control samples contained 2 μM Ero1-α(WT) or 10 μM PDI in the presence of 10 mM GSH. Oxidation of reduced PDI was initiated by the injection of 2 μM Ero1-α or Ero1-α(C104A/C131A) and was monitored with an oxygen electrode. (F) Schematic and representative diagrams of the active (O_{x1}) and inactive (O_{x2}) forms of Ero1-α and its constitutively active mutant Ero1-α(C104A/C131A).

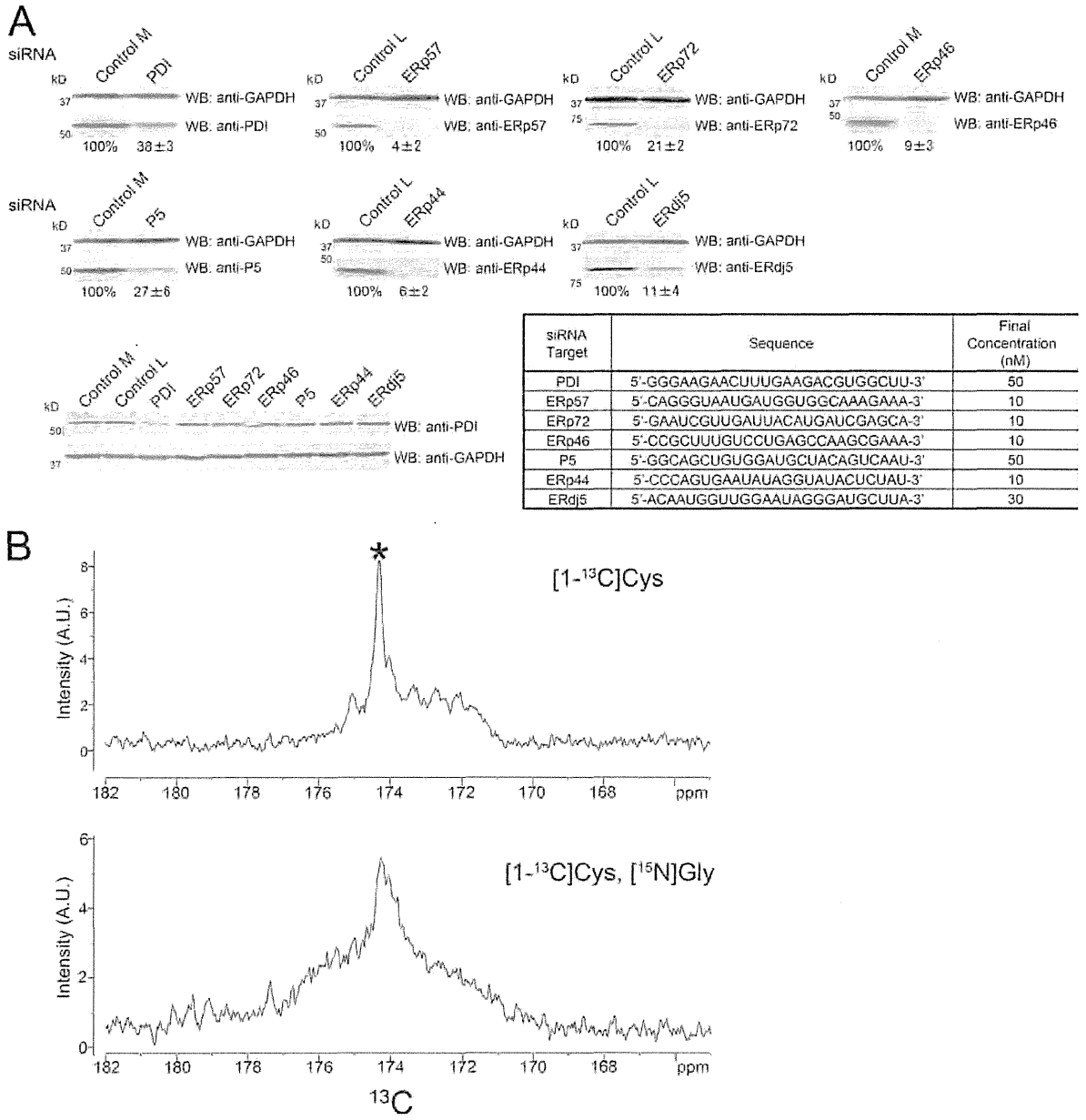

siRNA Target	Sequence	Final Concentration (nM)
PDI	5'-GGGAAGAACUUUGAAGACGUGGCUU-3'	50
ERp57	5'-CAGGGUAAUGAUGGUGGCAAAGAAA-3'	10
ERp72	5'-GAAUCGUUGAUUACAUGAUCGAGCA-3'	10
ERp46	5'-CCGCUUUGUCCUGAGCCAAGCGAAA-3'	10
P5	5'-GGCAGCUGUGGAUGCUACAGUCAAU-3'	50
ERp44	5'-CCCAGUGAAUAUAGGUAUACUCUAU-3'	10
ERdj5	5'-ACAAUGGUUGGAAUAGGGAUGCUUA-3'	30

Figure S2. **Validation of siRNA silencing and annotation of Cys94 with a double-labeling method.** (A) siRNA-mediated silencing in HEK293T cells was achieved via transfection of predesigned siRNAs. The sequences and concentrations are summarized in the bottom table. As controls, two different siRNAs (L, low GC content; M, medium GC content) were used, depending on the GC content of each siRNA. At 72 h after transfection, cell lysates were analyzed by SDS-PAGE and immunoblotted against the target protein and GAPDH. Endogenous expression levels of PDI under each siRNA silencing condition were detected as controls and are shown in the bottom row in A. Numbers below indicate knockdown efficiency. (B) ^{13}C NMR spectra of constitutively active Ero1-α, which was selectively labeled with ^{13}C at the carbonyl carbons of cysteine residues ([1-^{13}C]Cys; top) or both at [1-^{13}C]Cys and at the nitrogen of glycine residues ([^{15}N]Gly; bottom). The spectrum of the unlabeled protein has been subtracted. The asterisk indicates the peak originating from Cys94, which was significantly reduced after selective double labeling as a result of rapid transverse nuclear spin relaxation (Serve et al., 2010). WB, Western blot; A.U., arbitrary unit.

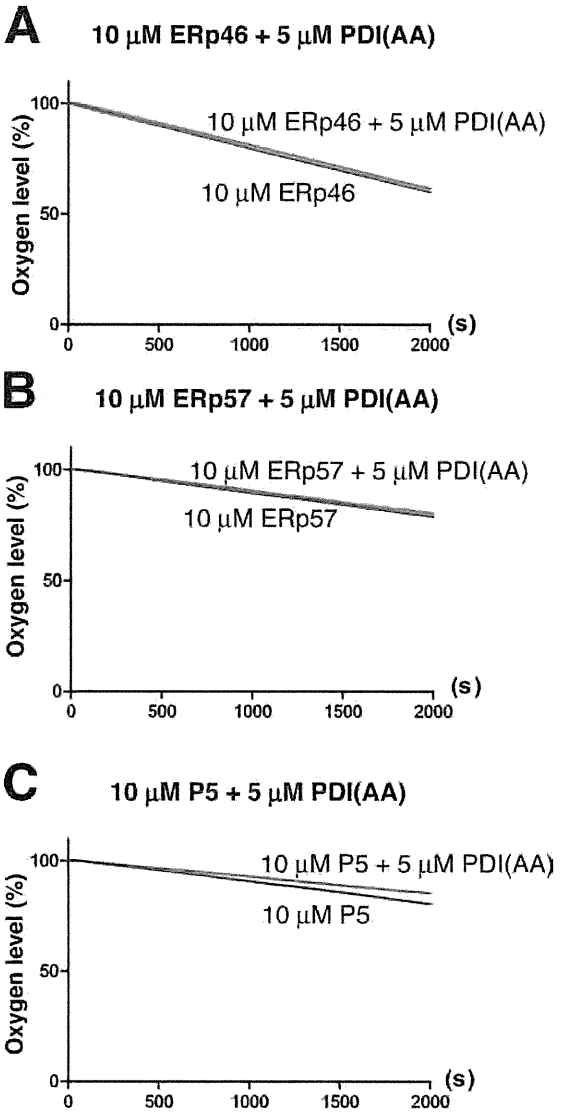

Figure S3. **PDI(AA) does not accelerate the Ero1-α oxidation system.** (A–C) Oxygen consumption was assayed in the presence of 10 mM GSH and 10 μM ERp46 (A), ERp57 (B), and P5 (C) either with or without 5 μM PDI(AA).

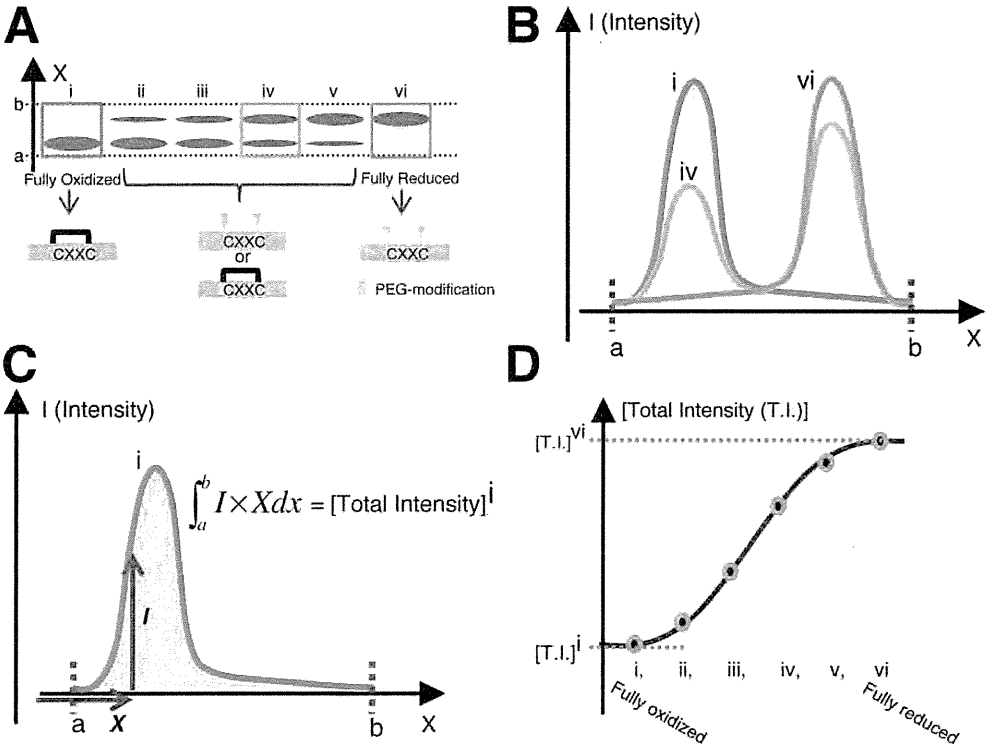

Figure S4. **Method used to calculate the K_{eq} values.** The following procedure was used to calculate the K_{eq} values from SDS-PAGE bands. To simplify the model, the redox protein containing one active domain is shown. (A) Free sulfhydryl groups on the cysteine residues were modified with mPEG2000-mal (molecular weight of 2,000) after incubation with different $[GSH]^2/[GSSG]$ ratios in a buffer containing GSSG and varying concentrations of GSH followed by SDS-PAGE and CBB staining. The active sites of the reduced form (vi, blue column) were modified with mPEG2000-mal. As a result, the reduced form migrated more slowly than the oxidized form. After CBB staining, the mean intensity of the horizontal pixels in each box was calculated along a line from the lower side of the fully oxidized form a to the upper side of the fully reduced form b using ImageJ (National Institutes of Health). (B) The x axis represents the longitudinal axis in A, and the y axis is the calculated mean pixel intensity. Total intensities were calculated using the integration shown in C. (D) For fitting, the values for the completely oxidized ($[T.I]^i$) or reduced state ($[T.I]^{vi}$) were regarded as 0 or 1, respectively, and all intermediate states were recalibrated as shown in Fig. 6 B.

Table S1. **List of publications reporting Ero1-α–related assays and having a bearing on this study**

Ero1-α–related assay	Figure in this study	Studies related to this study						Other studies
		PDI	ERp44	ERp57	ERp46	P5	ERp72	
Immunoprecipitation of Ero1-α (detecting WT oxidoreductase)	1 A, 6 A, and S1 A	Benham et al., 2000; Mezghrani et al., 2001; Anelli et al., 2002; Bertoli et al., 2004; Otsu et al., 2006; Appenzeller-Herzog et al., 2008, 2010; Masui et al., 2011; Benham et al., 2013	Anelli et al., 2002, 2003; Bertoli et al., 2004; Otsu et al., 2006	Appenzeller-Herzog et al., 2010			Appenzeller-Herzog et al., 2010	
Immunoprecipitation of the CXXA/AXXA mutant of oxidoreductase (detecting Ero1-α)	S1 B and 6 A	Jessop et al., 2009b; Schulman et al., 2010; Zito et al., 2010		Jessop et al., 2007, 2009a,b; Schulman et al., 2010	Jessop et al., 2009b	Jessop et al., 2009b; Schulman et al., 2010	Schulman et al., 2010	ERp18: Jessop et al., 2009b; ERp18, TMX, PDIR, and PDIp: Schulman et al., 2010
Activation of Ero1-α by oxidoreductase (e.g., detecting the $O_{x1}/(O_{x1} + O_{x2})$ ratio)	2, A and B	Otsu et al., 2006[a]; Appenzeller-Herzog et al., 2008	Otsu et al., 2006[a]	Appenzeller-Herzog et al., 2008				TMX3: Appenzeller-Herzog et al., 2008
In vitro oxidase assays (e.g., oxygen consumption assay and RNase assay)	1, D and E; and S1 E	Tsai and Rapoport, 2002; Baker et al., 2008; Wang et al., 2009; Chambers et al., 2010; Inaba et al., 2010; Zito et al., 2010; Araki and Nagata, 2011a; Masui et al., 2011; Wang et al., 2011	Not analyzed in this study[b]	Inaba et al., 2010				
In vitro binding assays (e.g., SPR assay and ITC measurements)	1 B and S1, C and D	Wang et al., 2009; Inaba et al., 2010; Araki and Nagata, 2011a; Masui et al., 2011	Masui et al., 2011	Inaba et al., 2010				

ITC, isothermal titration calorimetry.
[a]Otsu et al. (2006) examined the redox states of Ero1-α when PDI or ERp44 was overexpressed. However, at that time, the redox states of Ero1-α were unknown to correlate with its activation.
[b]Because ERp44 has a CRFS motif, it has no detectable redox activity. Hence, it was not listed under the oxygen consumption assay.

References

Anelli, T., M. Alessio, A. Mezghrani, T. Simmen, F. Talamo, A. Bachi, and R. Sitia. 2002. ERp44, a novel endoplasmic reticulum folding assistant of the thioredoxin family. *EMBO J.* 21:835–844. http://dx.doi.org/10.1093/emboj/21.4.835

Anelli, T., M. Alessio, A. Bachi, L. Bergamelli, G. Bertoli, S. Camerini, A. Mezghrani, E. Ruffato, T. Simmen, and R. Sitia. 2003. Thiol-mediated protein retention in the endoplasmic reticulum: the role of ERp44. *EMBO J.* 22:5015–5022. http://dx.doi.org/10.1093/emboj/cdg491

Appenzeller-Herzog, C., J. Riemer, B. Christensen, E.S. Sørensen, and L. Ellgaard. 2008. A novel disulphide switch mechanism in Ero1alpha balances ER oxidation in human cells. *EMBO J.* 27:2977–2987. http://dx.doi.org/10.1038/emboj.2008.202

Appenzeller-Herzog, C., J. Riemer, E. Zito, K.T. Chin, D. Ron, M. Spiess, and L. Ellgaard. 2010. Disulphide production by Ero1α-PDI relay is rapid and effectively regulated. *EMBO J.* 29:3318–3329. http://dx.doi.org/10.1038/emboj.2010.203

Araki, K., and K. Nagata. 2011a. Functional in vitro analysis of the ERO1 protein and protein-disulfide isomerase pathway. *J. Biol. Chem.* 286:32705–32712. http://dx.doi.org/10.1074/jbc.M111.227181

Baker, K.M., S. Chakravarthi, K.P. Langton, A.M. Sheppard, H. Lu, and N.J. Bulleid. 2008. Low reduction potential of Ero1alpha regulatory disulphides ensures tight control of substrate oxidation. *EMBO J.* 27:2988–2997. http://dx.doi.org/10.1038/emboj.2008.230

Benham, A.M., A. Cabibbo, A. Fassio, N. Bulleid, R. Sitia, and I. Braakman. 2000. The CXXCXXC motif determines the folding, structure and stability of human Ero1-Lalpha. *EMBO J.* 19:4493–4502. http://dx.doi.org/10.1093/emboj/19.17.4493

Benham, A.M., M. van Lith, R. Sitia, and I. Braakman. 2013. Ero1-PDI interactions, the response to redox flux and the implications for disulfide bond formation in the mammalian endoplasmic reticulum. *Philos. Trans. R. Soc. Lond. B Biol. Sci.* 368:20110403. http://dx.doi.org/10.1098/rstb.2011.0403

Bertoli, G., T. Simmen, T. Anelli, S.N. Molteni, R. Fesce, and R. Sitia. 2004. Two conserved cysteine triads in human Ero1alpha cooperate for efficient disulfide bond formation in the endoplasmic reticulum. *J. Biol. Chem.* 279:30047–30052. http://dx.doi.org/10.1074/jbc.M403192200

Chambers, J.E., T.J. Tavender, O.B. Oka, S. Warwood, D. Knight, and N.J. Bulleid. 2010. The reduction potential of the active site disulfides of human protein disulfide isomerase limits oxidation of the enzyme by Ero1α. *J. Biol. Chem.* 285:29200–29207. http://dx.doi.org/10.1074/jbc.M110.156596

Inaba, K., S. Masui, H. Iida, S. Vavassori, R. Sitia, and M. Suzuki. 2010. Crystal structures of human Ero1α reveal the mechanisms of regulated and targeted oxidation of PDI. *EMBO J.* 29:3330–3343. http://dx.doi.org/10.1038/emboj.2010.222

Jessop, C.E., S. Chakravarthi, N. Garbi, G.J. Hämmerling, S. Lovell, and N.J. Bulleid. 2007. ERp57 is essential for efficient folding of glycoproteins sharing common structural domains. *EMBO J.* 26:28–40. http://dx.doi.org/10.1038/sj.emboj.7601505

Jessop, C.E., T.J. Tavender, R.H. Watkins, J.E. Chambers, and N.J. Bulleid. 2009a. Substrate specificity of the oxidoreductase ERp57 is determined primarily by its interaction with calnexin and calreticulin. *J. Biol. Chem.* 284:2194–2202. http://dx.doi.org/10.1074/jbc.M808054200

Jessop, C.E., R.H. Watkins, J.J. Simmons, M. Tasab, and N.J. Bulleid. 2009b. Protein disulphide isomerase family members show distinct substrate specificity: P5 is targeted to BiP client proteins. *J. Cell Sci.* 122:4287–4295. http://dx.doi.org/10.1242/jcs.059154

Masui, S., S. Vavassori, C. Fagioli, R. Sitia, and K. Inaba. 2011. Molecular bases of cyclic and specific disulfide interchange between human ERO1alpha protein and protein-disulfide isomerase (PDI). *J. Biol. Chem.* 286:16261–16271. http://dx.doi.org/10.1074/jbc.M111.231357

Mezghrani, A., A. Fassio, A. Benham, T. Simmen, I. Braakman, and R. Sitia. 2001. Manipulation of oxidative protein folding and PDI redox state in mammalian cells. *EMBO J.* 20:6288–6296. http://dx.doi.org/10.1093/emboj/20.22.6288

Otsu, M., G. Bertoli, C. Fagioli, E. Guerini-Rocco, S. Nerini-Molteni, E. Ruffato, and R. Sitia. 2006. Dynamic retention of Ero1alpha and Ero1beta in the endoplasmic reticulum by interactions with PDI and ERp44. *Antioxid. Redox Signal.* 8:274–282. http://dx.doi.org/10.1089/ars.2006.8.274

Schulman, S., B. Wang, W. Li, and T.A. Rapoport. 2010. Vitamin K epoxide reductase prefers ER membrane-anchored thioredoxin-like redox partners. *Proc. Natl. Acad. Sci. USA.* 107:15027–15032. http://dx.doi.org/10.1073/pnas.1009972107

Serve, O., Y. Kamiya, A. Maeno, M. Nakano, C. Murakami, H. Sasakawa, Y. Yamaguchi, T. Harada, E. Kurimoto, M. Yagi-Utsumi, et al. 2010. Redox-dependent domain rearrangement of protein disulfide isomerase coupled with exposure of its substrate-binding hydrophobic surface. *J. Mol. Biol.* 396:361–374. http://dx.doi.org/10.1016/j.jmb.2009.11.049

Tsai, B., and T.A. Rapoport. 2002. Unfolded cholera toxin is transferred to the ER membrane and released from protein disulfide isomerase upon oxidation by Ero1. *J. Cell Biol.* 159:207–216. http://dx.doi.org/10.1083/jcb.200207120

Wang, L., S.J. Li, A. Sidhu, L. Zhu, Y. Liang, R.B. Freedman, and C.C. Wang. 2009. Reconstitution of human Ero1-Lalpha/protein-disulfide isomerase oxidative folding pathway in vitro. Position-dependent differences in role between the a and a' domains of protein-disulfide isomerase. *J. Biol. Chem.* 284:199–206. http://dx.doi.org/10.1074/jbc.M806645200

Wang, L., L. Zhu, and C.C. Wang. 2011. The endoplasmic reticulum sulfhydryl oxidase Ero1β drives efficient oxidative protein folding with loose regulation. *Biochem. J.* 434:113–121. http://dx.doi.org/10.1042/BJ20101357

Zito, E., E.P. Melo, Y. Yang, A. Wahlander, T.A. Neubert, and D. Ron. 2010. Oxidative protein folding by an endoplasmic reticulum-localized peroxiredoxin. *Mol. Cell.* 40:787–797. http://dx.doi.org/10.1016/j.molcel.2010.11.010

⌘ *Author's Choice*

THE JOURNAL OF BIOLOGICAL CHEMISTRY VOL. 288, NO. 41, pp. 29586–29594, October 11, 2013

Dynamic Regulation of Ero1α and Peroxiredoxin 4 Localization in the Secretory Pathway*[S]

Received for publication, March 8, 2013, and in revised form, August 23, 2013 Published, JBC Papers in Press, August 26, 2013, DOI 10.1074/jbc.M113.467845

Taichi Kakihana[‡§1], **Kazutaka Araki**[¶1], **Stefano Vavassori**[‖], **Shun-ichiro Iemura**[**], **Margherita Cortini**[‖], **Claudio Fagioli**[‖], **Tohru Natsume**[¶], **Roberto Sitia**[‖2,3], **and Kazuhiro Nagata**[§2,4]

From the [‡]*Department of Molecular and Cellular Biology, Institute for Frontier Medical Sciences, Kyoto University, 53 Kawahara-cho, Shogoin, Sakyo-ku, Kyoto 606-8397, Japan, the* [§]*Laboratory of Molecular and Cellular Biology, Faculty of Life Sciences, Kyoto Sangyo University, Motoyama, Kamigamo, Kita-ku, Kyoto 603-8555, Japan, the* [‖]*Università Vita-Salute San Raffaele Scientific Institute, Division of Genetics and Cell Biology, Via Olgettina 58, I-20132 Milan, Italy, the* [¶]*Molecular Profiling Research Center for Drug Discovery, National Institute of Advanced Industrial Science and Technology, 2-4-7 Aomi, Koto-ku, Tokyo 135-0064, Japan, and the* [**]*Medical Industry Translational Research Center, Fukushima Medical University, 1 Hikarigaoka, Fukushima 960-1295, Japan*

Background: Ero1α and peroxiredoxin 4 contribute to disulfide formation in the early secretory compartment (ESC), but lack known retention signals.
Results: Retention and localization of Ero1α and peroxiredoxin 4 are maintained through multistep and pH-dependent interactions with PDI and ERp44 in ESC.
Conclusion: PDI and ERp44 dynamically localize Ero1α and peroxiredoxin 4 in ESC.
Significance: The levels and localization of four interactors allow differential ESC redox control.

In the early secretory compartment (ESC), a network of chaperones and enzymes assists oxidative folding of nascent proteins. Ero1 flavoproteins oxidize protein disulfide isomerase (PDI), generating H_2O_2 as a byproduct. Peroxiredoxin 4 (Prx4) can utilize luminal H_2O_2 to oxidize PDI, thus favoring oxidative folding while limiting oxidative stress. Interestingly, neither ER oxidase contains known ER retention signal(s), raising the question of how cells prevent their secretion. Here we show that the two proteins share similar intracellular localization mechanisms. Their secretion is prevented by sequential interactions with PDI and ERp44, two resident proteins of the ESC-bearing KDEL-like motifs. PDI binds preferentially Ero1α, whereas ERp44 equally retains Ero1α and Prx4. The different binding properties of Ero1α and Prx4 increase the robustness of ER redox homeostasis.

Secretory or membrane proteins attain their native state in the ER,[5] under the assistance of a vast array of resident chaperones and enzymes. Formation, cleavage, or rearrangement of disulfide bond is catalyzed by oxidoreductases of the protein disulfide isomerase (PDI) family, which in humans lists over 20 members (1). The *CXXC* motifs in thioredoxin-like active domains, so-called a-domains, mediate disulfide interchange reactions. Redox-inactive domains, or b-domains, of similar structure but lacking *CXXC* motifs are frequently found in PDI family members. In PDI, for instance, the two redox-active domains (a- and a′-domain) are separated by the b- and b′-domains (a-b-b′-a′). The b′-domain provides a hydrophobic pocket onto which client proteins and ER oxidoreductin-1 (Ero1) molecules dock (2, 3).

ERp44 has an a-b-b′ domain organization (4) and plays important roles in the early secretory compartment (ESC) (5). Unlike PDI and other KDEL-bearing proteins, ERp44 accumulates in the ER-Golgi intermediate compartment (ERGIC) and cis Golgi (6, 7). In its a-domain, ERp44 has a conserved redox motif, CRFS, whose cysteine (Cys-29) is used to form mixed disulfides with IgM, adiponectin, and other client proteins for thiol-dependent quality control (8–10). ERp44 binds and regulates Ero1α and β, two key ESC-resident oxidases (11), and displays pH-dependent conformational change in ESC to prominently retrieve Ero1 and premature secretory proteins from the ERGIC to the ER (12).

Upon transferring disulfide bonds to incoming client proteins, PDI can be efficiently reoxidized by members of the Ero1 family (Ero1α and Ero1β in mammals). As these flavoproteins use oxygen as an electron acceptor generating hydrogen peroxide as a byproduct, the question arose as to how professional secretory cells could fold abundant proteins rich in disulfide bonds with limiting oxidative stress. A solution of this paradox came with the discovery that peroxiredoxin 4 (Prx4) can promote *de novo* disulfide bond formation by utilizing hydrogen peroxide (13, 14). Furthermore, it has been recently revealed

* This work was supported by Grant-in-aid for Scientific Research (S) 24227009 and a grant from the Human Frontier Science Program (HFSP) (to K. N.), by grants from Telethon (GGP11077) and the Associazione Italiana Ricerca Cancro (AIRC; IG and 5 x 1000 program) (to R. S.), and by Japan Society for the Promotion of Science (JSPS) Fellowships 08J03849 and 12J02049) (to K. A.) and 12J04142 (to T. K.).
⌘ *Author's Choice*—Final version full access.
[S] This article contains supplemental Figs. 1–5.
[1] Both authors contributed equally to this work.
[2] Both authors contributed equally to this work.
[3] To whom correspondence may be addressed. Tel.: 39-02-2643-4722; Fax: 39-02-2643-4723; E-mail: sitia.roberto@hsr.it.
[4] To whom correspondence may be addressed. Tel.: 81-75-705-3090; Fax: 81-75-705-3121; E-mail: nagata@cc.kyoto-su.ac.jp.
[5] The abbreviations used are: ER, endoplasmic reticulum; ERGIC, ER-Golgi intermediate compartment; Ero1, ER oxidoreductin-1; ESC, early secretory compartment; PDI, protein disulfide isomerase; Prx4, peroxiredoxin 4; roGFP, redox-sensitive green fluorescent protein; LC-MS/MS, liquid chromatography-tandem mass spectrometry.

that mice with double knock-out of both oxidases exhibit lower birth rate and scurvy, whereas mice with single knock-out (Ero1 or Prx4) exhibit modest effect, indicating mutual complementarity between Ero1 and Prx4 (15). Surprisingly, however, neither Prx4 nor Ero1 contains known ER retention signals (supplemental Fig. 1). Ero1α interacts with PDI and ERp44 (16) and to a minor extent with other family members, including ERp57, ERp46, ERp18, P5, and ERp72 (17–19) In line with their preferential binding, ERp44 and PDI can efficiently retain overexpressed Ero1α (20). On the other hand, it has been unclear how Prx4 is retained in the ER (21).

In this study, we investigated the mechanisms that control the intracellular localization of Prx4. Our findings reveal that Prx4 shares a similar stepwise retention mechanism with Ero1α, in which ERp44 functions as a backup for PDI; when PDI is down-regulated, Ero1α and Prx4 are retained by ERp44 in the downstream compartment of the ER. Such dynamic regulation of two main ER oxidases seems important for maintaining redox homeostasis in the ESC because the expression of Ero1α and Prx4 endowed with KDEL motifs caused hyperoxidizing environment in the ER.

EXPERIMENTAL PROCEDURES

Cells and Antibodies—HeLa and HEK293 cells were cultured in Dulbecco's modified Eagle's medium with 10% fetal bovine serum and antibiotics. The primary antibodies used in the experiments were: mouse monoclonal anti-GFP (Roche Applied Science, Basel, Switzerland), mouse monoclonal anti-HA (Cell Signaling Technology), mouse monoclonal and rabbit polyclonal anti-FLAG (Sigma-Aldrich), mouse monoclonal anti-Prx4 (Abcam, Cambridge, UK), mouse monoclonal anti-Ero1α (Abcam for Western blot and Santa Cruz Biotechnology for immunofluorescence), mouse monoclonal anti-β-actin (Millipore), mouse monoclonal anti-ERGIC53 (Enzo Chemical Laboratories), rabbit polyclonal anti-ERp46 (Santa Cruz Biotechnology), chicken polyclonal anti-P5 (Santa Cruz Biotechnology), rabbit polyclonal anti-PDI (StressGen Biotechnologies Corp.), rabbit polyclonal anti-ERp44 (reported by Ronzoni *et al.* (22)), rabbit polyclonal anti-ERp72 (Santa Cruz Biotechnology), and rabbit polyclonal calnexin (Cell Signaling). The secondary antibodies used in the experiments were: HRP-anti-rabbit IgG, HRP-anti-mouse IgG, Alexa Fluor 488 anti-rabbit or -mouse, and Alexa Fluor 546 anti-rabbit or -mouse (Invitrogen).

Construction of Plasmids—Human Prx4, PDI (wild type or AA mutant), or Ero1α (wild type or C94A mutant) cDNA with a FLAG tag or with a FLAG tag and KDEL sequence at the C terminus was generated by PCR from a Matchmaker Pretransformed Human HeLa library (Clontech) and subcloned into pcDNA3.1. The vectors for the expression of HA-ERp44-WT, C29S, and HA-ERp57 were as described previously (9). DsRed2-ER was purchased from Clontech. ERp44 C29A was generated by site-directed mutagenesis: (forward, 5′-GTA AAT TTT ATG CTG ACT GGG CTC GTT TCA GTC AGA TGT TGC-3′; reverse, GCA ACA TCT GAC TGA AAC GAG CCC AGT CAG CAT AAA AAT TTA C-3′). The ER-targeted redox-sensitive GFP iE variant (ERroGFPiE) was generated from ERroGFPiL (kind gift from Prof. Neil J. Bulleid) by site-directed mutagenesis: (forward, 5′-GGA ATA CAA CTA TAA CTG CGA AAG CAA TGT ATA CAT CAC GGC AG-3′; reverse, 5′-CTG CCG TGA TGT ATA CAT TGC TTT CGC AGT TAT AGT TGT ATT CC-3′).

Transfection, Secretion Assay, and Western Blot—Plasmids and siRNAs were transfected using Effectene® (Qiagen) or Lipofectamine RNAiMAX (Invitrogen), respectively, according to the manufacturer's instructions. For secretion assays, cells were incubated in Opti-MEM for an additional 4–6 h. Secreted materials were precipitated with 15% trichloroacetic acid (TCA) or immunoprecipitated with antibodies and then resolved by SDS-PAGE under reducing or nonreducing conditions. For detection of ERroGFPiE, lysates immunoprecipitated with anti-GFP were loaded. Fluorograms or Western blot images were acquired with the ChemiDoc-It imaging system (UVP, Upland, CA) or with the FLA-9000 Starion (Fujifilm Life Science) and quantified with ImageQuant 5.2 as described by Anelli *et al.* (7). Cells were extracted with 1% Nonidet P-40, 150 mM NaCl, 50 mM Tris-HCl (pH 8.0), and 20 mM *N*-ethylmaleimide. The detergent-soluble fractions of cell lysates were analyzed by Western blot.

Oligonucleotides—Stealth™ RNA siRNAs were obtained from Invitrogen. The sequences were as follows: siPDI-1, 5′-AAU GGG AGC CAA CUG UUU GCA GUG A-3′; siPDI-2, 5′-AUA AAG UCC AGC AGG UUC UCC UUG G-3′; siERp44-1, 5′-AUA GAG UAU ACC UAU AUU CAC UGG G-3′; siERp44-2, 5′-UUA AUU GCC GAG CUA CUU CAU UCU G-3′; and siEro1α, 5′-GGG CUU UAU CCA AAG UGU UAC CAU U-3′. Medium GC Stealth™ RNAi duplexes were used as negative controls.

LC-MS/MS Analysis—Immunoprecipitation was coupled with custom-made direct nano-flow liquid chromatography-tandem mass spectrometry system (Tokyo, Japan). FLAG-tagged Prx4 and mutants thereof were expressed in HEK293 cells and immunoprecipitated with anti-FLAG. Immunoprecipitates were eluted with FLAG peptides and digested with Lys-C endopeptidase (*Achromobacter* protease I). Cleaved fragments were directly analyzed by a direct nano-flow liquid chromatography-tandem mass spectrometry (LC-MS/MS) system as described previously (23). Assays were repeated at least four times.

Immunofluorescence—HeLa cells were washed with phosphate-buffered saline (PBS) and fixed with 4% paraformaldehyde for 20 min at room temperature. Cells were permeabilized with 0.2% Triton X-100 in PBS at room temperature for 5 min followed by incubation in 1% normal goat serum and 1% bovine serum albumin for 1 h. Cells were incubated with primary antibodies for 1 h and then with Alexa Fluor-conjugated secondary antibodies (from Invitrogen Molecular Probes) for 1 h, as indicated. Confocal images were obtained using a LSM 700 confocal microscope and analyzed by the Zen 2009 software (Carl Zeiss, Jena, Germany).

Preparation of Human Recombinant Prx4, Ero1α, PDI, and ERp44—Recombinant Ero1α and PDI were described previously (17, 24). Prx4 and ERp44 were expressed in *Escherichia coli* BL21 (DE3) cells (Novagen) by induction with 0.3 mM isopropyl-1-thio-β-D-galactopyranoside at 30 °C for 6 h just after the A_{600} reached 0.6. Harvested cells were sonicated in 20 mM HEPES (pH 7.5) containing 20 mM imidazole and 150 mM NaCl.

The supernatant from cell lysates was loaded onto a HisTrap column (GE Healthcare) equilibrated with cell suspension buffer and eluted with the same buffer containing 0.5 M imidazole. Eluted fractions were loaded onto a HiLoad 16/60 Superdex 200pg isofraction column equilibrated with 20 mM HEPES-NaOH (pH 7.5) containing 150 mM NaCl. Eluted fractions containing oxidoreductases were desalted and loaded onto a Resource Q column (GE Healthcare) equilibrated with 20 mM Tris-HCl (pH 8.0). Fractions were eluted by a linear gradient of NaCl. Purified proteins were concentrated and stored at −80 °C.

Surface Plasmon Resonance (SPR) Measurement—SPR analyses were performed as described previously (17, 24). Briefly, association or dissociation rate constants (k_{on} or k_{off}) to immobilized Ero1α (WT) or Prx4 were determined by SPR measurements on a ProteOn XPR36 protein interaction array system (Bio-Rad). Ero1α (WT)/Prx4 were coupled to the GLC sensor chip (Bio-Rad) through amine coupling chemistry. As a control, one channel was coupled with BSA to exclude background binding. Sensorgrams were recorded simultaneously for several concentrations (0.444–36 μM, in a 3-fold dilution series) of purified oxidoreductases at 25 °C for a 2-min association phase followed by a 10-min dissociation phase with 20 mM HEPES-NaOH (pH 7.4 or pH 6.4), 150 mM NaCl, 0.001% Tween, and 2 mM EDTA as running and sample buffer. Sensorgrams were analyzed by nonlinear regression analysis according to a two-state model by the ProteOn Manager version 3.0 software (Bio-Rad). Experiments were replicated at least three times.

Statistical Analysis—All data are presented as the means ± S.E. Statistical significance of the difference between groups was evaluated using Student's *t* test. $p < 0.05$ was considered significant. *, $p < 0.05$, **, $p < 0.01$, ***, $p < 0.001$.

Homologous Gene Analysis—To gain an evolutionary perspective, we searched and statistically analyzed homologous genes of ER oxidoreductases using the Kyoto Encyclopedia of Genes and Genomes (KEGG) database (25). The National Center for Biotechnology Information (NCBI) database was also searched for analysis of several sequences (www.ncbi.nlm.nih.gov/protein/).

RESULTS

Interactions of Prx4 and Ero1α with PDI Family Proteins—The ER oxidases Ero1α and Prx4 have at least two common features; one is their function in oxidative protein folding, and the other is their lack of intrinsic ER retention signals. Surprisingly, the latter feature is 100% conserved among Ero1α orthologs and 94.4% conserved among Prx4 in vertebrates (KEGG database (25)) (supplemental Fig. 1). To identify proteins involved in its subcellular localization, we performed LC-MS/MS analyses of the material co-immunoprecipitated with FLAG-tagged Prx4 and identified ERp44, PDI, ERp72, ERp46, and P5 (supplemental Fig. 2) (see also Ref. 18), yielding a pattern similar to what is reported for Ero1α. To further compare the interactomes of the two enzymes and provide additional specificity controls, we overexpressed Prx4-FLAG or Ero1α-FLAG in HeLa cells and analyzed the immunoprecipitates obtained with or without prior cross-linking with dithiobis succinimidyl propionate. Western blot analyses of the material specifically eluted with FLAG peptides confirmed that both Prx4 and Ero1α interact with ERp44, PDI, ERp72, P5, and ERp46 (Fig. 1*A*). The similar binding patterns are in line with coordinated roles of Prx4 and Ero1α in oxidative protein folding (26).

To confirm that endogenous ERp44 and Prx4 interact in physiological conditions, we analyzed Ig-λ producing J558L murine myeloma cells or a transfectant secreting IgM (J[μ_s] (27)). Clearly, endogenous Prx4 can be co-immunoprecipitated with ERp44 in Ig-secreting cells (Fig. 1*B*).

Next, we investigated whether Ero1α and Prx4 co-localize with ERp44 or PDI by immunofluorescence (Fig. 1*C*). Although PDI is primarily localized in the ER, endogenous ERp44 recycles between the ER and cis Golgi and accumulates preferentially in the ERGIC (6, 7). Consistent with the results shown in Fig. 1*A*, both Ero1α and Prx4 showed co-localization with PDI and ERp44 in HeLa cells (Fig. 1C). Co-localization was stronger with PDI, suggesting that Ero1α and Prx4 were mainly localized in the ER and to a lesser extent in the ERGIC. In many cells, co-staining with ERp44 and PDI was more evident for Prx4 than Ero1α (data not shown), which may reflect the localization of part of Ero1α in mitochondria-associated ER membranes (28, 29).

Secretion of Overexpressed Prx4 Is Inhibited by ERp44 and PDI—Confirming previous observations (30), overexpressed Prx4 was clearly secreted by HeLa cells (Fig. 2*A*, *lane 2*), implying that saturable mechanisms determine its intracellular retention. Co-expression of ERp44 or PDI, but not of ERp57, restored retention of overexpressed Prx4 (Fig. 2*A*, *lanes 3–5*). These secretory phenotypes were similar for Ero1α (Fig. 2*B*). In the experiment shown, ERp57 partly inhibited secretion of overexpressed Ero1α, albeit much less efficiently than ERp44 or PDI (Fig. 2*B*, *lane 5*) (20). ERp57 cooperates with calnexin and calreticulin to promote glycoprotein folding. The absence of glycosylation sites in Prx4 may explain why co-expressed ERp57 did not affect its secretion. Thus, ERp44 and PDI but not ERp57 can retain overexpressed Prx4.

In thiol-dependent quality control, Cys-29 in the atypical redox-active motif of ERp44 forms mixed disulfides with Ero1 and client proteins such as IgM, adiponectin, or SUMF1/FGE (sulfatase-modifying factor 1/formylglycine-generating enzyme) (5). Clearly, Prx4-FLAG secretion was decreased in a dose-dependent manner by wild type HA-ERp44 (WT) but not by a mutant in which Cys-29 was replaced by a serine (yielding ERp44 C29S, Fig. 2*C*). In contrast, a PDI mutant in which cysteine residues of the two *CXXC* motifs were replaced by alanine residues (PDI-AA) inhibited Prx4 secretion almost as efficiently as wild type molecules (Fig. 2*D*). Thus, the enzymatically active cysteine residues of PDI are not necessary for retention of Prx4.

Because Prx4 shares similar retention mechanisms with Ero1α, the two proteins could compete with each other. Accordingly, secretion of Prx4-FLAG was dramatically increased by Ero1α-FLAG co-expression (Fig. 2*E*, compare *lanes 2* and *4*). Also an enzymatically inactive mutant of Ero1α (Ero1α-C94A) promoted Prx4 secretion (Fig. 2*E*, *lane 5*). Conversely, secretion of Ero1α-FLAG was not increased by co-expression of abundant Prx4-FLAG (Fig. 2*F*, *lanes 2* and *4*).

PDI Preferentially Retains Ero1α, whereas ERp44 Equally Retains Ero1α and Prx4—The unidirectional competition between Ero1α and Prx4 suggested that the former binds to its retainers more efficiently than the latter. Therefore, we ana-

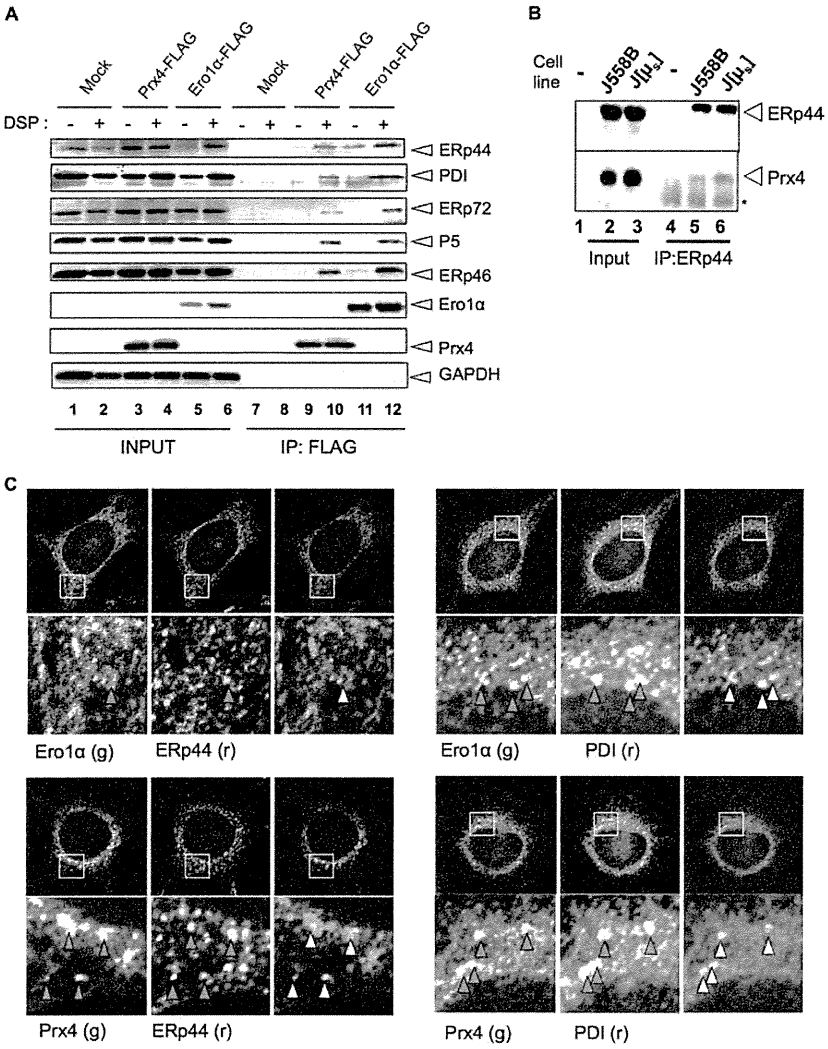

FIGURE 1. **Prx4 and Ero1α share similar partners and subcellular localizations.** *A*, 24 h after transfection with pcDNA3.1, Prx4-FLAG, or Ero1α-FLAG, 10^6 HeLa cells were incubated with or without 0.25 μM dithiobis succinimidyl propionate (*DSP*) on ice. Anti-FLAG immunoprecipitates (*IP*) were then eluted by FLAG peptides and analyzed by Western blot with the indicated antibodies. Aliquots of the total Nonidet P-40 lysates from 10^4 cells (*INPUT*) were loaded to estimate (co)-immunoprecipitation efficiency. *B*, lysates from 10^7 mouse myeloma J558L cells or their derivative expressing nitrophenol-specific secretory Ig-μ chains (*J[μs]*) were immunoprecipitated with anti-ERp44 and analyzed by Western blot with the indicated antibodies. The slightly more abundant Prx4 associated to ERp44 in J[μ_s] cells may reflect physiological interactions in the presence of an abundant substrate (7). *C*, HeLa cells were fixed by 4% paraformaldehyde and permeabilized by 0.2% Triton X-100. Co-localization of Prx4 or Ero1α with PDI or ERp44 was observed by immunofluorescence using the indicated fluorochrome-conjugated antibodies, as described under "Experimental Procedures." *g*, green. *r*, red.

lyzed their binding properties *in vitro* by surface plasmon resonance (SPR) assays and estimated the k_{on}, k_{off}, and K_D values. PDI bound Ero1α with ~5.5-fold stronger affinity than Prx4 at pH 7.4, which is similar to the pH in the ER (1.94 and 10.6 μM, respectively, Fig. 3*A* and supplemental Fig. 3). In contrast, the two enzymes displayed similar affinities for ERp44 at pH 6.4 (5.15 and 6.92 μM, for Ero1α and Prx4, respectively). The affinity of ERp44 to Ero1α and Prx4 was decreased at pH 7.4 in comparison with that at pH 6.4 (Fig. 3*A* and supplemental Fig. 3), suggesting that ERp44 binds Prx4 more effectively at low pH like in the distal ESC stations (10.4 and 17.9 μM for Ero1α and Prx4, respectively) (12). Extrapolating these *in vitro* results to the cellular environment, PDI would preferentially retain Ero1α in the ER.

To challenge this possibility, we co-expressed increasing amounts of PDI-FLAG with constant levels of Ero1α-FLAG and Prx4-FLAG in HeLa cells. 24 h after transfection, culture media and cell lysates were analyzed by Western blot (Fig. 3*B*) and quantified (Fig. 3*D*). Consistent with the *in vitro* results shown in Fig. 3*A*, Ero1α secretion was primarily inhibited by PDI, whereas higher levels of expression of PDI were required to retain Prx4 (Fig. 3, *B* and *D*). In contrast, HA-ERp44 inhibited secretion of Ero1α-FLAG and Prx4-FLAG to similar extents. Collectively, these results indicate that PDI binds and retains Ero1α more efficiently than Prx4.

Sequential Interactions of Ero1α and Prx4 with PDI and ERp44 in ESC—In view of their different distributions along ESC (7, 8), PDI and ERp44 might exert sequential effects on the

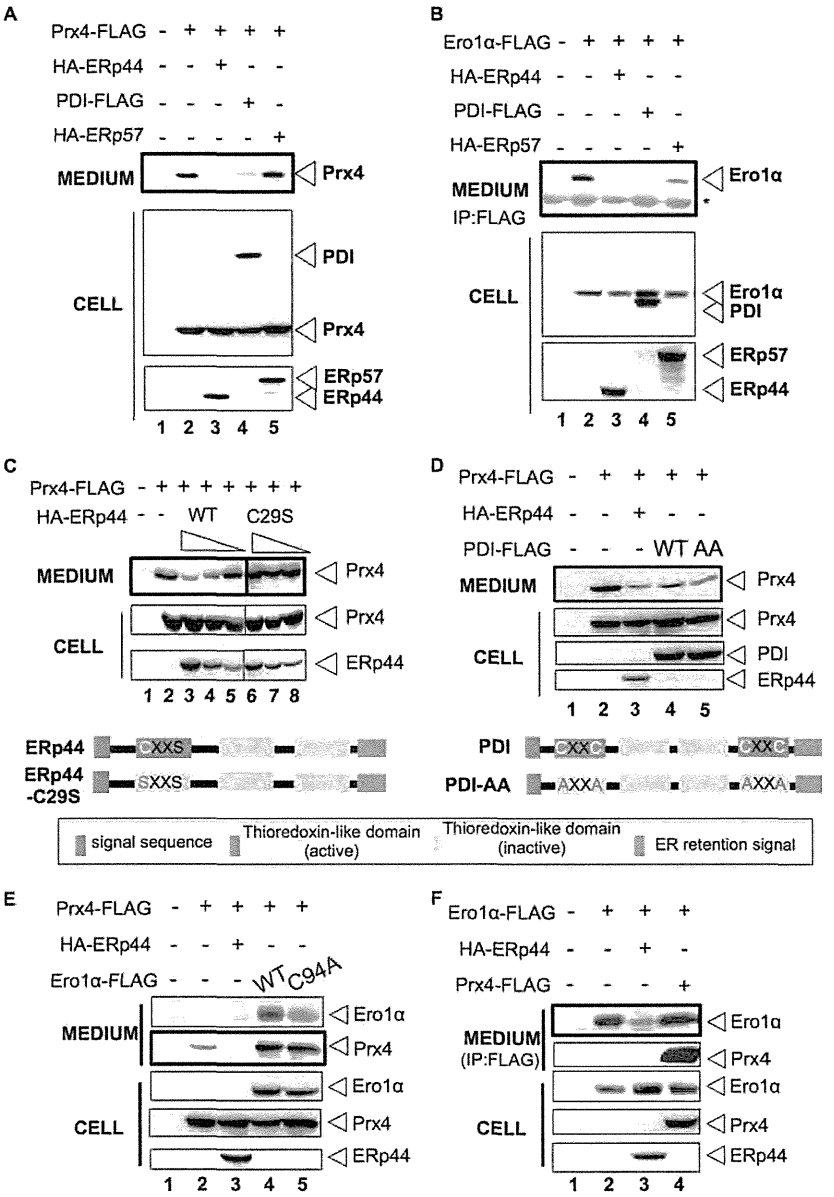

FIGURE 2. **Dynamic retention of Prx4 by ERp44 and PDI.** *A* and *B*, HeLa cells were co-transfected with Prx4-FLAG (*A*) or Ero1α-FLAG (*B*) and HA-ERp44, PDI-FLAG, or HA-ERp57 as indicated. 24 h after transfection, cells were cultured in FBS-free Opti-MEM medium for 5 h. The spent medium was subsequently precipitated with 15% TCA (*A*) or anti-FLAG antibodies (*B*) and analyzed by Western blot with the indicated antibodies. *C*, Prx4-FLAG was co-expressed in HeLa cells with increasing amounts of HA-ERp44-WT or the C29S mutant (9). 24 h after transfection, cells were handled as described for *panels A* and *B*. When compared with cells overexpressing Prx4-FLAG alone (*lane 2*), Prx4 secretion was inhibited by high levels of ERp44-WT (*lanes 3–5*) but not by ERp44-C29S (*lanes 6–8*). *D*, wild type (PDI-WT-FLAG) or a mutant PDI (PDI-AA-FLAG) in which all four cysteines in the a- and a′-domains had been mutated to alanine were co-expressed with Prx4-FLAG in HeLa cells and handled as above. When compared with cells overexpressing Prx4-FLAG alone (*lane 2*), both PDI-WT and the AA mutant retained Prx4 (*lanes 4* and *5*). *E* and *F*, wild type (Ero1α-FLAG) or an enzymatically inactive variant (Ero1α-C94A-FLAG) was co-expressed with Prx4 in HeLa cells. Clearly, Prx4 secretion was dramatically increased by co-expression of either Ero1α-FLAG or Ero1α-C94A-FLAG. In the experiment shown in *panel F*, Prx4-FLAG was co-expressed with Ero1α-FLAG in HeLa cells. Unlike what observed in *panel E*, retention of Ero1α was not competed by Prx4-FLAG co-expression.

localization/retention of Ero1α and Prx4. Therefore, we compared the effects of silencing ERp44, PDI, or both on the secretion of endogenous Prx4 and Ero1α by HeLa cells (Fig. 4*A*). Individual siRNAs for ERp44 or PDI effectively silenced the respective targets (Fig. 4*A*, *lanes 7–12*, *right panel*). Lowering the levels of ERp44 greatly promoted secretion of endogenous Prx4 (Fig. 4*A*, *lanes 1–3*, *upper*), but only marginally affected Ero1α retention (Fig. 4*A*, *lanes 1–3*, *lower*, and Fig. 4*C*, *upper*). Thus, under physiological conditions, PDI seems to retain Ero1α sufficiently. Neither endogenous Prx4 nor Ero1α was released by lowering the levels of PDI alone in HeLa cells (Fig. 4*A*, *lanes 4* and *5*, and Fig. 4*C*, *middle*). Considering that ERp44 is localized downstream with respect to PDI in the ESC, we surmised that ERp44 acted as a backup retention machinery in

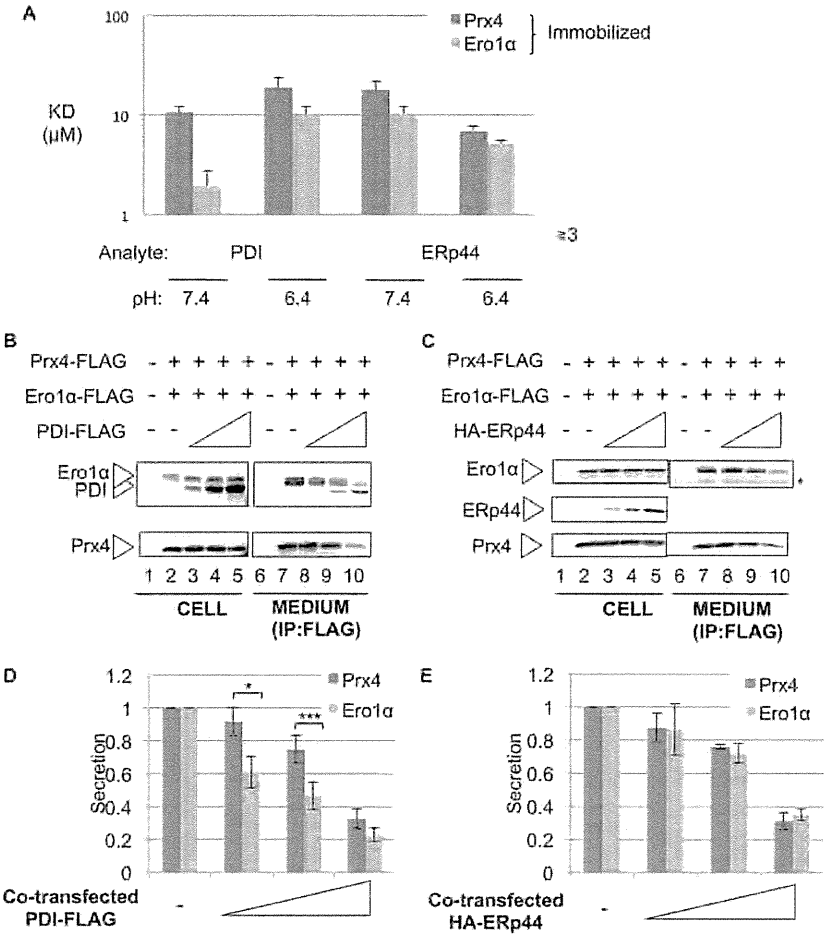

FIGURE 3. **Ero1α competes with Prx4 for PDI but not for ERp44 binding.** *A*, purified human Ero1α or Prx4 proteins were immobilized on a biosensor chip, and PDI or ERp44 was injected as analyte. The affinity of PDI for Ero1α is about 5.5-fold stronger than Prx4, whereas ERp44 interacts similarly with Ero1α or Prx4. *B–E*, Prx4-FLAG and Ero1α-FLAG were co-expressed with increasing amounts of PDI-FLAG (*B* and *D*) or HA-ERp44 (*C* and *E*) in HeLa cells. 24 h after transfection, cells were cultured in Opti-MEM for 4 h. Aliquots from cell lysates or anti-FLAG immunoprecipitates (*IP*) from the spent medium were analyzed by Western blotting (*D* and *E*) and quantified by densitometry. $n = 3$. *, $p < 0.05$, ***, $p < 0.001$.

the absence of PDI (Fig. 4*C*, *middle*). Accordingly, the simultaneous silencing of ERp44 and PDI allowed secretion of both endogenous Ero1α and endogenous Prx4 by HeLa cells (Fig. 4*A*, *lane 6*). Backup mechanism by ERp44 was further confirmed by immunofluorescence of HeLa cells transfected with nonspecific siRNA or specific PDI. Endogenous PDI was efficiently silenced by RNAi (supplemental Fig. 4). As expected, co-localization of ERp44 with Ero1α and Prx4 was increased in PDI-silenced cells (Fig. 5*B*), whereas such a condition did not affect the morphology of the ER or ERGIC (supplemental Fig. 4), suggesting that retention of Ero1α and Prx4 in ESC depends mostly on ERp44 in the absence of PDI. Thus, sequential interactions with PDI and ERp44 underlie the intracellular retention of Prx4 and Ero1α. Ero1α displays higher affinity for PDI, but in its absence, it can be retrieved by ERp44. On the other hand, Prx4 is mainly retained by ERp44 because of its lower affinity for PDI (Fig. 3*A*).

Lack of ER Retention Signals in Two ER Oxidases Is Important for ER Redox Homeostasis—In virtually all vertebrates, Ero1α and Prx4 do not harbor ER retention signals (25) (supplemental Fig. 1). As Ero1α and Prx4 play major roles in oxidative protein folding, we surmised that the stepwise retention/localization mechanism of these two ER oxidases in higher eukaryotes may be important for ER redox regulation. To monitor ER redox balance, therefore, we exploited ERroGFPiE. This sensor co-localized with ER-targeted DsRed2 (supplemental Fig. 5). As shown by Birk *et al.* (31), ERroGFPiE can be resolved into two bands under nonreducing conditions corresponding to its reduced (*i.e.* DTT-treated) and oxidized (*i.e.* dipyridyl disulfide-treated) isoforms (Fig. 5*A*, *lanes 2–4*). As indicated by the accumulation of reduced ERroGFPiE and consistent with the notion that Ero1α is a prominent ER oxidase, its knockdown caused hypo-oxidizing condition in the ER (Fig. 5*A*, *lane 7*). Next, we monitored the ER redox state in cells expressing KDEL-extended or wild type Ero1α. Surprisingly, expression of Ero1α-KDEL caused a more oxidizing shift in ERroGFPiE than wild type Ero1α (Fig. 5*A*, *lanes 5* and *6*). Similar results were obtained appending a KDEL motif to Prx4 (Fig. 5*B*). The co-expression of Ero1α with Prx4-KDEL caused a much more dramatic oxidative shift to the redox balance in the ER (Fig. 5*B*, *lane 6*). Taken together, our results strongly suggest that the

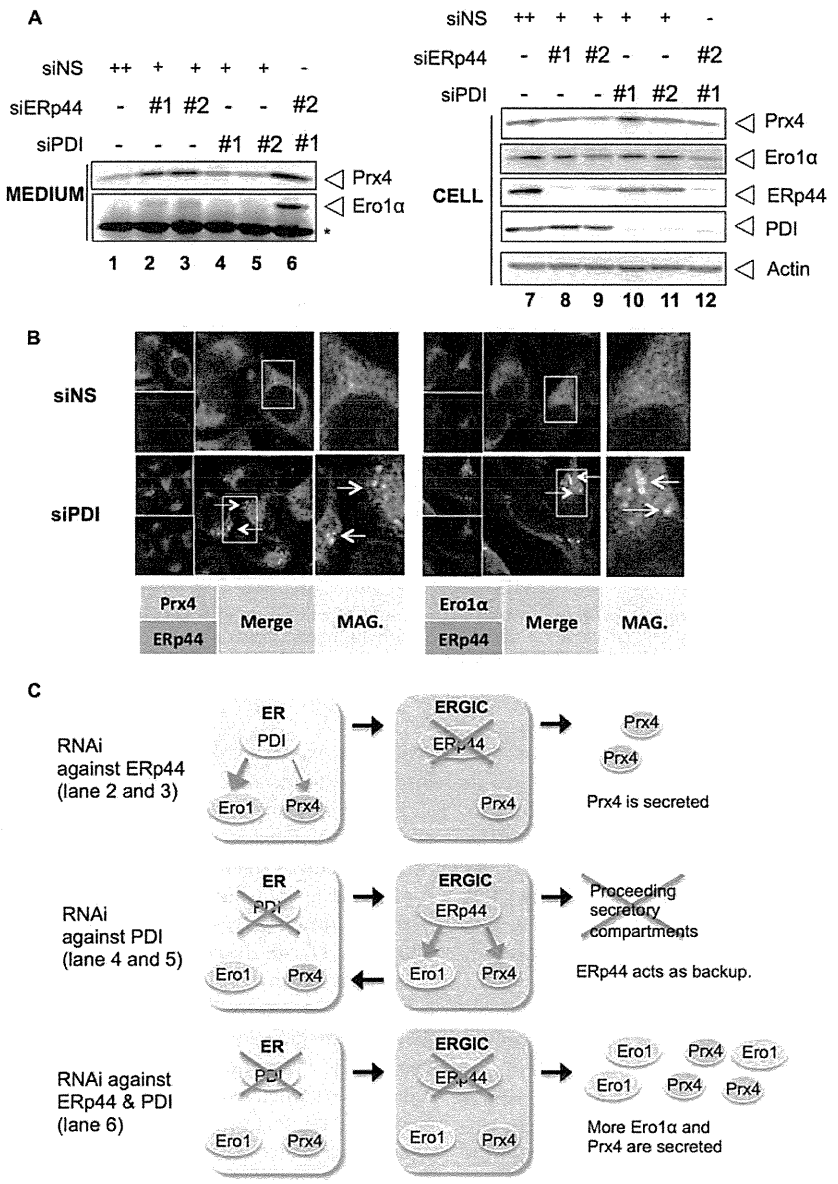

FIGURE 4. **Silencing ERp44 allows secretion of endogenous Prx4, but not Ero1α.** *A*, secretion of endogenous Prx4 or Ero1α by HeLa cells was analyzed with RNAi for nonspecific (*NS*) ERp44 or PDI (*lanes 1–5*) or both (*lane 6*) by specific siRNAs. 72 h after transfection, cells were cultured in Opti-MEM for 6 h and analyzed as described in the legend for Fig. 2. *B*, immunofluorescence of HeLa cells transfected with nonspecific siRNA (*siNS*) or PDI siRNA (*siPDI*). Endogenous Prx4 or Ero1α was co-stained with endogenous ERp44. In PDI-silenced cells the co-localization of Prx4 or Ero1α with ERp44 was more intense, consistent with a backup role of ERp44. *siERp44*, ERp44 siRNA. *C*, strategy utilized to dissect the retention of Ero1α and Prx4.

dynamic, stepwise retention mechanisms of Ero1α and Prx4 are important for fine-tuning the redox status along the ESC.

DISCUSSION

Our studies have established that two ER oxidases, Ero1α and Prx4, share a noncanonical retention mechanism in the ER. Knockdown of PDI exerted little effect on the secretion of Ero1α and Prx4, whereas knockdown of ERp44 allowed secretion of endogenous Prx4. This observation suggests that Prx4 retention is controlled mainly by ERp44 under physiological conditions. On the other hand, knockdown of both ERp44 and PDI caused marked secretion of Ero1α and Prx4. The different affinity of PDI for Ero1α and Prx4 partially explains why the former was mainly retained by PDI in the ER. After PDI knockdown, the localization of both Ero1α and Prx4 was changed from an ER pattern to a more vesicular pattern containing ERp44. Taken together, these observations strongly suggest that Ero1α and Prx4 are mainly retained by PDI in the proximal ESC. Because of its lower affinity for PDI, some Prx4 continuously reaches the distal ESC stations, from which it is retrieved by ERp44 in a pH-dependent manner, as described for overexpressed Ero1α or IgM subunits (12). In this scenario, ERp44

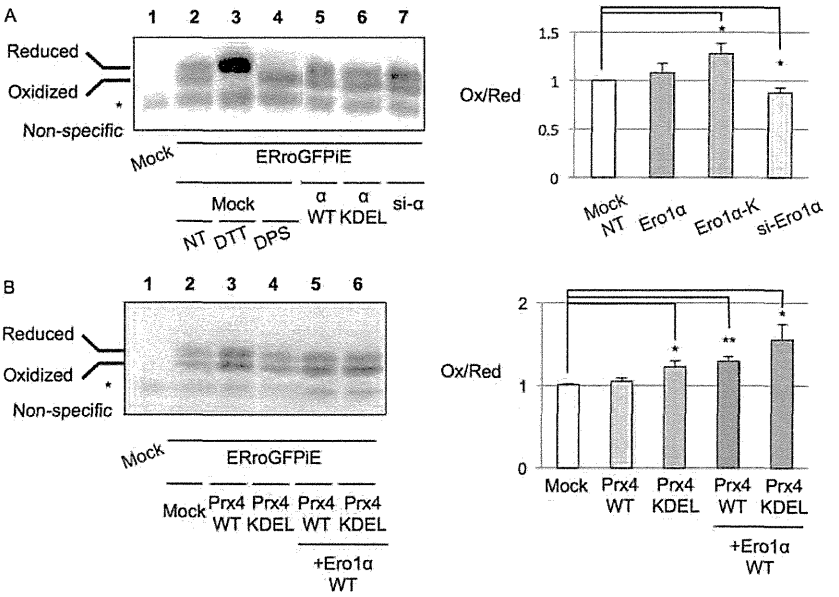

FIGURE 5. **Increased oxidation of ERroGFPiE upon co-expression of Ero1αKDEL and/or Prx4KDEL.** *A* and *B*, ERroGFPiE is transiently overexpressed in HeLa cells. Reductive or oxidative shift in the ER redox of cells indicated was detected in nonreducing Western blot and quantified. The average ratios of intensity of the oxidized band to the reduced band are depicted in graphs, which are standardized by the ratio of samples of nontreated (*NT*) cells (*lane 2*). $n = 3$. *, $p < 0.05$, **, $p < 0.01$. *DPS*, dipyridyl disulfide; *si-α*, Ero1α siRNA; *si-Ero1α*, Ero1α siRNA; *Ox/Red*, oxidized/reduced.

acts as a backup system. This multistep retention seems conserved throughout evolution; indeed, almost all vertebrates so far reported lack KDEL-like motifs (supplemental Fig. 1).

It is noteworthy that appending KDEL-like motifs to Ero1α or Prx4 caused hyperoxidizing conditions in the ER (Fig. 5). As suitable redox homeostasis is required for efficient as well as accurate oxidative protein folding in the ER (26), our results argue in favor of a physiological role for the dynamic retention of the two ESC oxidases.

An important result emerging from our studies is that ERp44 binds Prx4 more strongly at acidic pH. ERp44 is a unique PDI family member whose conserved CRFS active motif limits its potential function as an oxidoreductase. As a chaperone cycling in ESC, ERp44 preferentially binds its client proteins in the acidic environment of cis Golgi to retrieve them into the ER (12). Its lower affinity at neutral pH likely favors client release in the ER.

Because of their similar interaction patterns, Ero1α and Prx4 largely co-localize; their vicinity may optimize productive folding while limiting H_2O_2 production and oxidative stress. However, H_2O_2 is not only a foe, but can be utilized as an intra- or intercellular signaling device (32, 33). Therefore, it will be of interest to determine whether the relative levels of Ero1α, Prx4, and their retainer molecules differ between cell types or differentiation states. Besides its key potential role in maintaining redox homeostasis, the dynamic retention mechanism of Ero1α and Prx4 appears to generate a gradient of the two oxidases within the ESC. Considering its possible regulation by pH, such a gradient might have relevant functional consequences. Ero1α has been detected on platelet surface in association with PDI, where it might regulate integrin function (34). Particularly in cells establishing close contacts (*i.e.* immunological or neural synapses), export of redox-active molecules might regulate the intensity and duration of intercellular cross-talks.

The thiol group (-SH) of peroxidatic cysteine is oxidized by H_2O_2 to sulfenic acid (-SOH). At higher concentrations, H_2O_2 further oxidizes the sulfenic moieties to sulfinic ($-SO_2H$) and then sulfonic acid ($-SO_3H$). Prx4 can undergo hyperoxidation in the ER lumen (35); however, no sulfiredoxin activity has been detected so far in the secretory compartment. Therefore, sulfinylated or sulfonylated Prx4 is likely degraded or released, perhaps acting as intercellular signals. Prx4 is retained by thiol-dependent mechanisms (Fig. 1*C*), and modifications of the peroxidatic cysteines might lead to secretion. However, Prx4 release was similar in cells overexpressing wild type Ero1α or an enzymatically inactive mutant (Fig. 2*E*), suggesting that Ero1α does not weaken Prx4 retention via H_2O_2 production, but likely via competitive binding. However, additional H_2O_2 sources may cause Prx4 hyperoxidation and release (15). It should be important and interesting to examine whether and how the interactive retention mode of Ero1α and Prx4 regulates oxidative folding of nascent proteins and whether and how it can adapt to changing physiological requirements.

Acknowledgment—We thank Dr. Neil J. Bulleid for the generous gift of construct of ERroGFPiL.

REFERENCES

1. Hatahet, F., and Ruddock, L. W. (2009) Protein disulfide isomerase: a critical evaluation of its function in disulfide bond formation. *Antioxid. Redox Signal.* **11,** 2807–2850
2. Inaba, K., Masui, S., Iida, H., Vavassori, S., Sitia, R., and Suzuki, M. (2010) Crystal structures of human Ero1α reveal the mechanisms of regulated and targeted oxidation of PDI. *EMBO J.* **29,** 3330–3343

3. Masui, S., Vavassori, S., Fagioli, C., Sitia, R., and Inaba, K. (2011) Molecular bases of cyclic and specific disulfide interchange between human ERO1α protein and protein-disulfide isomerase (PDI). *J. Biol. Chem.* **286,** 16261–16271
4. Wang, L., Wang, L., Vavassori, S., Li, S., Ke, H., Anelli, T., Degano, M., Ronzoni, R., Sitia, R., Sun, F., and Wang, C. C. (2008) Crystal structure of human ERp44 shows a dynamic functional modulation by its carboxy-terminal tail. *EMBO Rep.* **9,** 642–647
5. Cortini, M., and Sitia, R. (2010) From antibodies to adiponectin: role of ERp44 in sizing and timing protein secretion. *Diabetes Obes. Metab.* **12,** Suppl. 2, 39–47
6. Gilchrist, A., Au, C. E., Hiding, J., Bell, A. W., Fernandez-Rodriguez, J., Lesimple, S., Nagaya, H., Roy, L., Gosline, S. J., Hallett, M., Paiement, J., Kearney, R. E., Nilsson, T., and Bergeron, J. J. (2006) Quantitative proteomics analysis of the secretory pathway. *Cell* **127,** 1265–1281
7. Anelli, T., Ceppi, S., Bergamelli, L., Cortini, M., Masciarelli, S., Valetti, C., and Sitia, R. (2007) Sequential steps and checkpoints in the early exocytic compartment during secretory IgM biogenesis. *EMBO J.* **26,** 4177–4188
8. Fraldi, A., Zito, E., Annunziata, F., Lombardi, A., Cozzolino, M., Monti, M., Spampanato, C., Ballabio, A., Pucci, P., Sitia, R., and Cosma, M. P. (2008) Multistep, sequential control of the trafficking and function of the multiple sulfatase deficiency gene product, SUMF1 by PDI, ERGIC-53 and ERp44. *Hum. Mol. Genet.* **17,** 2610–2621
9. Anelli, T., Alessio, M., Bachi, A., Bergamelli, L., Bertoli, G., Camerini, S., Mezghrani, A., Ruffato, E., Simmen, T., and Sitia, R. (2003) Thiol-mediated protein retention in the endoplasmic reticulum: the role of ERp44. *EMBO J.* **22,** 5015–5022
10. Wang, Z. V., Schraw, T. D., Kim, J. Y., Khan, T., Rajala, M. W., Follenzi, A., and Scherer, P. E. (2007) Secretion of the adipocyte-specific secretory protein adiponectin critically depends on thiol-mediated protein retention. *Mol. Cell. Biol.* **27,** 3716–3731
11. Araki, K., and Inaba, K. (2012) Structure, mechanism, and evolution of Ero1 family enzymes. *Antioxid. Redox Signal.* **16,** 790–799
12. Vavassori, S., Cortini, M., Masui, S., Sannino, S., Anelli, T., Caserta, I. R., Fagioli, C., Mossuto, M. F., Fornili, A., van Anken, E., Degano, M., Inaba, K., and Sitia, R. (2013) A pH-regulated quality control cycle for surveillance of secretory protein assembly. *Mol. Cell* **50,** 783–792
13. Zito, E., Melo, E. P., Yang, Y., Wahlander, Å., Neubert, T. A., and Ron, D. (2010) Oxidative protein folding by an endoplasmic reticulum-localized peroxiredoxin. *Mol. Cell* **40,** 787–797
14. Tavender, T. J., Springate, J. J., and Bulleid, N. J. (2010) Recycling of peroxiredoxin IV provides a novel pathway for disulphide formation in the endoplasmic reticulum. *EMBO J.* **29,** 4185–4197
15. Zito, E., Hansen, H. G., Yeo, G. S., Fujii, J., and Ron, D. (2012) Endoplasmic reticulum thiol oxidase deficiency leads to ascorbic acid depletion and noncanonical scurvy in mice. *Mol. Cell* **48,** 39–51
16. Mezghrani, A., Fassio, A., Benham, A., Simmen, T., Braakman, I., and Sitia, R. (2001) Manipulation of oxidative protein folding and PDI redox state in mammalian cells. *EMBO J.* **20,** 6288–6296
17. Araki, K., Iemura, S., Kamiya, Y., Ron, D., Kato, K., Natsume, T., and Nagata, K. (2013) *J. Cell Biol.* **202,** 861–874
18. Jessop, C. E., Watkins, R. H., Simmons, J. J., Tasab, M., and Bulleid, N. J. (2009) Protein disulphide isomerase family members show distinct substrate specificity: P5 is targeted to BiP client proteins. *J. Cell Sci.* **122,** 4287–4295
19. Appenzeller-Herzog, C., Riemer, J., Zito, E., Chin, K. T., Ron, D., Spiess, M., and Ellgaard, L. (2010) Disulphide production by Ero1α-PDI relay is rapid and effectively regulated. *EMBO J.* **29,** 3318–3329
20. Otsu, M., Bertoli, G., Fagioli, C., Guerini-Rocco, E., Nerini-Molteni, S., Ruffato, E., and Sitia, R. (2006) Dynamic retention of Ero1α and Ero1β in the endoplasmic reticulum by interactions with PDI and ERp44. *Antioxid. Redox Signal.* **8,** 274–282
21. Kakihana, T., Nagata, K., and Sitia, R. (2012) Peroxides and peroxidases in the endoplasmic reticulum: integrating redox homeostasis and oxidative folding. *Antioxid. Redox Signal.* **16,** 763–771
22. Ronzoni, R., Anelli, T., Brunati, M., Cortini, M., Fagioli, C., and Sitia, R. (2010) Pathogenesis of ER storage disorders: modulating Russell body biogenesis by altering proximal and distal quality control. *Traffic* **11,** 947–957
23. Natsume, T., Yamauchi, Y., Nakayama, H., Shinkawa, T., Yanagida, M., Takahashi, N., and Isobe, T. (2002) A direct nanoflow liquid chromatography-tandem mass spectrometry system for interaction proteomics. *Anal. Chem.* **74,** 4725–4733
24. Araki, K., and Nagata, K. (2011) Functional *in vitro* analysis of the ERO1 protein and protein-disulfide isomerase pathway. *J. Biol. Chem.* **286,** 32705–32712
25. Kanehisa, M., and Goto, S. (2000) KEGG: Kyoto Encyclopedia of Genes and Genomes. *Nucleic Acids Res.* **28,** 27–30
26. Zito, E. (2013) PRDX4, an endoplasmic reticulum-localized peroxiredoxin at the crossroads between enzymatic oxidative protein folding and nonenzymatic protein oxidation. *Antioxid. Redox Signal.* **18,** 1666–1674
27. Fagioli, C., Mezghrani, A., and Sitia, R. (2001) Reduction of interchain disulfide bonds precedes the dislocation of Ig-μ chains from the endoplasmic reticulum to the cytosol for proteasomal degradation. *J. Biol. Chem.* **276,** 40962–40967
28. Anelli, T., Bergamelli, L., Margittai, E., Rimessi, A., Fagioli, C., Malgaroli, A., Pinton, P., Ripamonti, M., Rizzuto, R., and Sitia, R. (2012) Ero1α regulates Ca^{2+} fluxes at the endoplasmic reticulum-mitochondria interface (MAM). *Antioxid. Redox Signal.* **16,** 1077–1087
29. Gilady, S. Y., Bui, M., Lynes, E. M., Benson, M. D., Watts, R., Vance, J. E., and Simmen, T. (2010) Ero1α requires oxidizing and normoxic conditions to localize to the mitochondria-associated membrane (MAM). *Cell Stress Chaperones* **15,** 619–629
30. Okado-Matsumoto, A., Matsumoto, A., Fujii, J., and Taniguchi, N. (2000) Peroxiredoxin IV is a secretable protein with heparin-binding properties under reduced conditions. *J. Biochem.* **127,** 493–501
31. Birk, J., Meyer, M., Aller, I., Hansen, H. G., Odermatt, A., Dick, T. P., Meyer, A. J., and Appenzeller-Herzog, C. (2013) Endoplasmic reticulum: reduced and oxidized glutathione revisited. *J. Cell Sci.* **126,** 1604–1617
32. Bae, Y. S., Oh, H., Rhee, S. G., and Yoo, Y. D. (2011) Regulation of reactive oxygen species generation in cell signaling. *Mol. Cells* **32,** 491–509
33. Niethammer, P., Grabher, C., Look, A. T., and Mitchison, T. J. (2009) A tissue-scale gradient of hydrogen peroxide mediates rapid wound detection in zebrafish. *Nature* **459,** 996–999
34. Swiatkowska, M., Padula, G., Michalec, L., Stasiak, M., Skurzynski, S., and Cierniewski, C. S. (2010) Ero1α is expressed on blood platelets in association with protein-disulfide isomerase and contributes to redox-controlled remodeling of αIIbβ3. *J. Biol. Chem.* **285,** 29874–29883
35. Tavender, T. J., and Bulleid, N. J. (2010) Peroxiredoxin IV protects cells from oxidative stress by removing H_2O_2 produced during disulphide formation. *J. Cell Sci.* **123,** 2672–2679

MCB
Journals ASM.org

The Casein Kinase 2-Nrf1 Axis Controls the Clearance of Ubiquitinated Proteins by Regulating Proteasome Gene Expression

Yoshiki Tsuchiya,[a] Hiroaki Taniguchi,[a] Yoshiyuki Ito,[a] Tomoko Morita,[a] M. Rezaul Karim,[a] Norihito Ohtake,[a] Kousuke Fukagai,[a] Takao Ito,[a] Shota Okamuro,[a] Shun-ichiro Iemura,[b] Tohru Natsume,[b] Eisuke Nishida,[c] Akira Kobayashi[a]

Laboratory for Genetic Code, Graduate School of Life and Medical Sciences, Doshisha University, Kyotanabe, Japan[a]; National Institutes of Advanced Industrial Science and Technology, Biological Information Research Center (JBIRC), Kohtoh-ku, Tokyo, Japan[b]; Department of Cell and Developmental Biology, Graduate School of Biostudies, Kyoto University, Kyoto, Japan[c]

Impairment of the ubiquitin-proteasome system (UPS) has been implicated in the pathogenesis of human diseases, including neurodegenerative disorders. Thus, stimulating proteasome activity is a promising strategy to ameliorate these age-related diseases. Here we show that the protein kinase casein kinase 2 (CK2) regulates the transcriptional activity of Nrf1 to control the expression of the proteasome genes and thus the clearance of ubiquitinated proteins. We identify CK2 as an Nrf1-binding protein and find that the knockdown of CK2 enhances the Nrf1-dependent expression of the proteasome subunit genes. Real-time monitoring of proteasome activity reveals that CK2 knockdown alleviates the accumulation of ubiquitinated proteins upon proteasome inhibition. Furthermore, we identify Ser 497 of Nrf1 as the CK2 phosphorylation site and demonstrate that its alanine substitution (S497A) augments the transcriptional activity of Nrf1 and mitigates proteasome dysfunction and the formation of p62-positive juxtanuclear inclusion bodies upon proteasome inhibition. These results indicate that the CK2-mediated phosphorylation of Nrf1 suppresses the proteasome gene expression and activity and thus suggest that the CK2-Nrf1 axis is a potential therapeutic target for diseases associated with UPS impairment.

Accumulation of misfolded and ubiquitinated proteins is a common pathological feature of various human diseases, such as amyotrophic lateral sclerosis (ALS), inclusion body myopathies, alcoholic and nonalcoholic steatohepatitis, and neurodegenerative disorders, including Alzheimer's, Parkinson's, and Huntington's disease (1–3). Multiple lines of evidence suggest that both the ubiquitin-proteasome system (UPS) and autophagy are responsible for the clearance of ubiquitinated proteins that would accumulate in these age-related diseases. It has been demonstrated that the 26S proteasome can degrade soluble ubiquitinated proteins but not the insoluble aggregates, which are targeted by the autophagy-lysosome pathway (4–7). Impairment of proteasome activity is known to cause proteins that are normally turned over by the UPS to aggregate and form inclusion bodies. Thus, it is expected that the upregulation of proteasome activity could prevent inclusion body formation and mitigate the progression of neurodegenerative and related diseases that are caused by the accumulation of abnormal proteins.

Nrf1 (nuclear factor E2-related factor 1 or Nfe2l1) is a member of the Cap'n'Collar (CNC) family of basic leucine zipper (bZip) transcription factors, which also includes p45 NF-E2, Nrf2, and Nrf3 (8, 9). Nrf1 regulates its target gene expression through either the antioxidant response element (ARE) or the Maf recognition element (MARE) by heterodimerizing with small Maf proteins (8, 9). Several gene targeting studies have implicated Nrf1 in the regulation of cellular homeostasis in embryos, hepatocytes, and osteoclasts (10–14). Recent studies have revealed that Nrf1 also plays an essential role in maintaining neuronal cells and that the loss of Nrf1 induces neurodegeneration and abnormal accumulation of ubiquitinated protein aggregates in neurons (15, 16). The impairment of protein homeostasis that is induced by Nrf1 deficiency may be due to the decreased expression of proteasome subunits in these neurons (16). Indeed, Nrf1 controls the expression of proteasome subunit genes in mammalian cells under proteasome dysfunction (17, 18). Therefore, it is critically important to reveal the role of Nrf1 in the regulation of proteasome gene expression and to elucidate the molecular mechanisms underlying the regulation of Nrf1 activity.

In this study, we reveal that the vast majority of proteasome subunit genes and some proteasome-associated genes are under the transcriptional control of Nrf1. We identify the protein kinase casein kinase 2 (CK2) as an Nrf1-interacting protein and demonstrate that CK2 controls proteasome gene expression and activity by suppressing the transcriptional activity of Nrf1. A mutation of the CK2 phosphorylation site of Nrf1 enhances the proteasome activity and reduces the formation of juxtanuclear inclusion bodies. Thus, our work proposes that the CK2-Nrf1 axis could be a new regulatory target for the efficient clearance of ubiquitinated proteins.

MATERIALS AND METHODS

Antibodies. The antibodies utilized in this study were normal rabbit IgG (Santa Cruz), anti-Flag (M2; Sigma), anti-α-tubulin (DM1A; Sigma), antihemagglutinin (anti-HA) (Y-11; Santa Cruz), anti-green fluorescent protein (anti-GFP) (B-2; Santa Cruz), anti-Nrf1 (H-285; Santa Cruz), anti-MafK (C-16; Santa Cruz), anti-CK2α (1AD9; Santa Cruz), anti-CK2α′ (ab10474; Abcam), anti-CK2β (6D5; Santa Cruz), anti-p62/

Received 15 September 2012 Returned for modification 10 October 2012
Accepted 6 June 2013
Published ahead of print 1 July 2013
Address correspondence to Akira Kobayashi, akobayas@mail.doshisha.ac.jp.
M.R.K., N.O., K.F., T.I., and S.O. contributed equally to this work.
Supplemental material for this article may be found at http://dx.doi.org/10.1128/MCB.01271-12.

doi:10.1128/MCB.01271-12